THE DETERMINATION OF CRUSTAL STRUCTURE IN THE ADELAIDE GEOSYNCLINE USING QUARRY BLASTS AS SEISMIC SOURCES

by

P. R. J. Shackleford

B. Sc. Hons. (Adelaide)

A Thesis

Submitted for the Degree of

Master of Science

in the

Department of Physics

University of Adelaide

1978

Awarded March 1979

TABLE OF CONTENTS

SUMMARY

This thesis describes a seismic experiment, the aim of which was to determine a model of the crust for South Australia in the region of the Adelaide geosyncline, in terms of the variation of seismic velocity with depth, down to the Mohorovicic Discontinuity. Chemical explosions at three large open cut mining operations were used as sources of seismic energy for recording along three linear profiles directed along and approximately transverse to the north-south axis of the geosyncline.

The first chapter contains a review of seismic experiments conducted previously in South Australia, together with a resumé of other geophysical experiments which have bearing on the crustal-mantle structure in the Adelaide geosyncline.

Chapter two describes the experimental procedures which were adopted for the present seismic survey. This includes descriptions of the recording equipment, the choice of recording sites, the method of determining the times of blasting at each quarry and a description of each blast source.

Stations of the permanent seismic network, which is operated by the University of Adelaide, recorded seismic arrivals from the three blast sources. The travel times of seismic waves from the sources to the permanent stations are discussed in Chapter three. An attempt is made to

obtain a model of the crust based on these travel times to the permanent stations, for comparison with crustal models deduced by earlier workers from essentially the same station network. The results of the present study are significantly different from crustal models determined previously from earthquake data.

Chapter four contains the experimental results obtained from the three seismic profiles, and their interpretation. The resultant crustal model, which is the simplest model consistent with the observed travel times, consists of two essentially homogeneous crustal layers overlying the mantle. The average P wave velocities in the upper and lower crustal layers are 5.95 km/s and 6.46 km/s respectively, with the boundary between these layers occurring at a depth of approximately 18 km. The P wave velocity in the upper mantle is 7.97 km/s. The mean thickness of the crust is 39 km. Both the intermediate and Moho discontinuities vary by up to 5 km from their mean depths. Shear waves have velocities of 3.43 and 4.45 km/sec in the upper crustal layer and the upper mantle respectively.

Appendix A reviews the theoretical basis of seismic interpretation in large scale refraction surveys, and briefly considers alternative approaches to the seismic inversion problem. Appendix B contains the travel times of seismic phases observed on the temporary station networks.

DECLARATION

To the best of the author's knowledge and belief, this thesis contains no material which has been accepted for the award of any other degree or diploma in any University, and no material previously published or written by another person, except where due reference is made.

P. R. J. Shackleford

ACKNOWLEDGEMENTS

Thanks are due to Dr. S.I. Evans, Director of the South Australian Institute of Technology, where the author was a member of staff, for permission to undertake the work, and to Dr. G.L. Goodwin, Head of the School of Physics.

The author is also indebted to Dr. D.J. Sutton and the staff of the Seismology Section of the Physics Dept of the University of Adelaide for their advice and practical assistance in the collection of seismic records.

The job of the scientist is to invent a story which accounts for a set of observations, and then decide how likely that story is.

B. Kinsman

CHAPTER 1

REVIEW OF PREVIOUS STUDIES OF THE CRUST AND UPPER MANTLE IN SOUTH AUSTRALIA

1.1 Seismic Determinations of Crustal Structure in South Australia

The first attempt to determine the crustal structure in Southern Australia was made in 1956 by way of an unreversed refraction profile from the atomic test site at Maralinga, west along the trans-continental railway to a distance of $\Delta = 11^{o}$ (Bolt, Doyle & Sutton (1958)). Seismic phases Pn, Sn, P_1 and S_1 were recorded and their velocities determined (Table 1.1). The travel times of the observed phases were found to be consistent with a crustal model having a single layer over the mantle. There was no evidence of any intracrustal layering. The single recording station to the south east of Maralinga, at Adelaide ($\Delta = 7.85^{o}$) gave large positive residuals, corresponding to arrivals which were 2.7s, 5.2s and 2.3s later than expected for the phases Pn, Sn and S_1, respectively. The values of crustal thickness which were determined, for the single layered crustal model are shown in Table 1.2.

A second series of atomic tests in 1957 was used to record seismic wave arrivals at four stations south east of Maralinga across Eyre Peninsula, toward Adelaide (Doyle and Everingham (1964)). The P and S wave mantle velocities (Table 1.1) can be seen to be lower than those resulting

Table 1.1 Seismic Velocities for South Australian Crust and Upper Mantle

Survey	seismic velocities (km/s)			
	P_1	Pn	S_1	Sn
Bolt, Doyle, Sutton (1958)	6.03±0.09	8.21±0.005	3.55±0.04	4.75±0.01
Doyle & Everingham (1964)	6.3	8.05±0.04	3.59±0.01	4.61±0.04
White (1969)	6.23	8.06	3.58*	4.63
White (1969)		8.05		
White (1969)	6.2		3.6	
White (1969)		7.92±0.03		
Hawkins et al (1965)	6.26			
Stewart (1971)	6.24±0.02	7.99±0.02	3.58±0.01	4.58±0.02
Stewart (revised)	6.25±0.03	8.02±0.03	3.58±0.01	4.56±0.02
Finlayson et al (1974)	P_1 6.2*	8.04±0.04		
	P_2 6.7*			

* assumed values for analysis

Table 1.2 Estimates of Crustal Thickness

SURVEY		DEPTH (km)	REGION
BDS	refraction profile (unreversed)	32 (P-data)	West from Maralinga
		39 (S-data)	
DE	"	39±4 (P-data)	S-E from Maralinga
		37 (reflections)	
White (1969)	local earthquake data	38±6	Range and graben area
Stewart (1971)	"	35±2	" " "
Stewart (1972)	"	37±1 (small variations)	" " "

from the earlier study. This difference was attributed to real upper mantle differences between the two regions surveyed, rather than to a Moho dipping consistently over a distance of 2000 km. It was also shown by this survey that the anomalous travel times observed at Adelaide in the earlier experiment were explained by the lower seismic velocities found to exist on Eyre Peninsula in the second experiment, rather than to seismic anomalous crustal structure in the so-called Adelaide "shatter belt", as may have been supposed from the observations of the first survey alone. Again there was no need to invoke an intermediate layer to explain observed phases, but records at distances where such phases may have been evident were described as being not of sufficiently good quality to enable small later phases to be read. Two phases which may have arisen from an intermediate refractor were interpreted as Moho reflections. This study, like the first, was along an unreversed profile. Crustal depths (Table 1.2) were determined from both Pn data and from some near vertically reflected phases.

In 1960, the Lamont Geological Observatory's ship VEMA made several seismic refraction traverses off the Australian coast, one of which was over the South Australian shelf. This work is reported in detail by Hawkins et al (1965). Their determination of a basement P velocity of 6.26 km/sec on the shelf (Table 1.1) was in agreement with the value determined earlier by Doyle and Everingham for the crustal velocity across Eyre Peninsula.

In the mid 1960's, White (1969) carried out an analysis for seismic velocities and crustal thickness in South Australia, based on local earthquake data from the University of Adelaide's permanent seismic station network (hereafter termed the permanent network). He assumed a crustal model consisting of a uniform single layered crust over the mantle, one velocity value (S_1), and a minimum depth of focus for the earthquakes. The values (Tables 1.1 and 1.2) which he obtained for the remaining velocities and crustal thickness agreed with the values determined by Doyle and Everingham. Although White used local earthquake data, his analysis did not depend on accurate epicentral determinations, but he did presuppose uniformity of crustal structure over the region encompassed by the seismic network.

Additional work, using information from local earthquakes, was done by Stewart (1971, 1972) who, in a treatment of local earthquake residuals obtained on the basis of White's (1969) crustal model, corrected White's model by solving a set of residual equations for correction terms in the crustal and epicentral parameters, for 473 phases from 52 earthquakes. By also allowing for low velocity cover rocks at the recording sites, and a possible velocity gradient in the crystalline basement, he determined station correction terms which, when included with his original residual analysis, produced a marginally different structure from that of White. By interpreting station residuals in terms of variations of Moho depth, Stewart found a possible

thinning of the crust in the Spencer-St Vincent gulf regions, and a thickening of up to 3 km in the region between latitudes 34^{o} to 35^{o} S.

A third large scale seismic experiment was conducted in South Australia when, during 1972 the Bureau of Mineral Resources detonated three large explosions as energy sources for seismic refraction observations. The results have been reported by Finlayson et al (1974). One blast was located at the Mt. Fitton South Copper Mine in the north Flinders Ranges. Records were obtained at all South Australian permanent seismic stations, and in particular, at the three stations Partacoona (PNA), Hallett (HTT) and Adelaide (ADE), which are situated south of Mt. Fitton, roughly along the axis of the Adelaide geosyncline. The Pn velocity obtained from this unreversed profile agreed with the values found by Doyle and Everingham, Stewart and White. A second blast at Kunanalling in Western Australia afforded the opportunity to record a reversed profile between it and the Mt. Fitton blast. The travel times, together with those from Maralinga, were analysed by the time-depth method of Hawkins (1961), and Moho depths were calculated for a two layered crust consisting of an upper layer 20 km thick with a P_1 velocity of 6.2 km/s, which was underlain by the lower crust with P velocity of 6.7 km/s. Time depth analysis then enabled a linear map of crustal thickness to be determined along the east-west profile. This map showed a thickening of the crust from west to east, with depths ranging from 41 to 49 km in the Adelaide Geosyncline region, and 39 to 40 km under the

eastern part of the Nullabor shield. This later observation agreed with that of Doyle and Everingham.

An earlier major detonation was that at the Ord Dam site in northern Australia. The results of a seismic experiment based on this blast were presented by Denham et al (1972). When travel times from the Ord Dam explosion were combined with those from the Mt. Fitton shot to stations situated north of Mt. Fitton, and records from the Adelaide Geosyncline region were also included, Finlayson et al found that the north-south travel times were consistent with a Moho velocity of 7.96 km/s at 40 km, with a further increase in velocity to 8.18 km/s at a depth of 61 km. The 8.18 km/s material, which appeared to be a sub-Moho refractor in the Central Australian region, was thought to be continuous with the sub-basement material beneath the Shield.

1.2 Comments

From these studies and their results, it could be concluded that the crust in South Australia is single layered and homogeneous, with a thickness of approximately 38 km. It will be noted, however, that no detailed refraction studies of the crust had been made, and that the two crustal studies which had been conducted in the geosyncline region, were based on local earthquake data. The data for these studies were derived from an assumed crustal model, and necessarily contained uncertainties in both hypocentral

location and origin time. Furthermore, as White (1967) has pointed out, the resolving power of seismic methods for intra-crustal layering depends on the predominant wavelength used. Kosminskaya and Riznichenko (1964) have suggested that layers about five wavelengths thick can be accurately distinguished with densely placed seismographs. Given the predominant wavelength of 2 to 3 km recorded by the South Australian permanent stations, and the large distances between stations, the averaging of crustal fine structure in previous studies based on data from earthquake sources, can be understood.

The single long range refraction "profile" recorded south from Mt. Fitton along the geosyncline was unreversed, as have been the other large scale refraction surveys in South Australia, with the exception of the Kunanalling-Mt. Fitton and the Ord Dam-Mt. Fitton "traverses" (see above). The Mount Fitton profile, however, was unable to offer any clarification of the crustal structure in the geosyncline because the large distances between stations meant that crustal phases were only recorded as late arrivals, with the exception of the arrival at Umberatana at a distance of 49.2 km from Mt. Fitton.

1.3 Other Geophysical Studies

In addition to those seismic studies already mentioned, which have been concerned specifically with the South Australian crust and upper mantle, a number of other studies

and experiments have been carried out which provide significant information for the modelling of the crustal structure in South Australia. These studies have been summarized in part or in whole by Dooley (1970), Cleary (1973) and Finlayson et al (1974). Some of the studies describe Australia-wide geophysical trends, and in this regard have emphasized the significance of the Adelaide Geosyncline in this broader context, as an eastern boundary to the Australian Precambrian Shield.

Gutenberg and Richter (1954), in their study of world wide seismicity, associated the South Australian seismic zone with the eastern margin of the Australian Precambrian Shield, and identified it as an intermediate zone between the old shield and the recently tectonically active area of eastern Australia.

The change of structure which occurs in the upper mantle along an east-west profile, roughly in the region of the Adelaide geosyncline, has been studied more recently by, for example, Cleary, Simpson and Muirhead (1972) and McElhinny (1973). In the first of these studies Cleary et al determined station anomalies for several Australian seismic stations that recorded arrivals from the Cannikin nuclear explosion in the Aleutian Islands, 1971. Cleary et al attributed the trend observed in the station anomalies to the presence of a low velocity layer in the upper mantle, so that negative station anomalies over much of the Shield area indicated a poorly developed low velocity layer (LVL),

whilst the positive anomalies to the east were thought to be due to a well developed LVL. A plot of station anomaly against longitude revealed that the most rapid change from positive to negative anomaly coincided approximately with the Adelaide Geosyncline. This was interpreted as resulting from a wedging out of the upper mantle low velocity layer as the shield boundary was approached. This interpretation was supported by McElhinny and followed the interpretation given to similar results in North America by Hales and Doyle (1967). The decline of the LVL westward has been attributed to the ageing of the upper mantle. The idea of an older mantle in the Shield region is also supported by heat flow measurements which are higher to the east and in the South Australian seismic zone than they are over the Shield to the west (Jaeger (1970)).

In an attempt to explain the distribution of Australian seismicity using plate tectonic theory, Cleary and Simpson (1971) suggested that the South Australian seismic zone might mark a boundary between sub-plates of the Indo-Australian plate, which are rifting apart. First motion studies for South Australian earthquakes should enable a distinction to be made between the tensional or compressional nature of the forces acting in the S.A. seismic zone. Stewart (1972) favoured tensional forces after studying a small number of local earthquakes.

In addition to the studies mentioned above which are almost exclusively seismic-based studies, Gough et al (1974)

established a magnetometer array across the geosyncline, north of Port Augusta. From the observed magnetic field variations, an electrical conductivity anomaly was located in the crust or upper mantle. The long curved conductor was found to run north-south, approximately parallel to the geosyncline axis, and slightly eastward of the seismic zone. It was suggested that the anomalous region occurs in the lower crust or upper mantle, and three possible explanations of the anomaly were proposed. It was suggested that the conductor may be associated with recent tectonic activity, in which case it may signify high mantle temperatures corresponding to an upwelling of mantle material into the lower crust. (This hypothesis is in accord with the active rift concept of Cleary and Simpson (1971) and Stewart (1972)); the conductor may coincide with an ancient fracture zone postulated by Cook (1966), Wilson (1968) and Crawford (1970) independently of any seismic information; thirdly, the conductor may represent an easterly remnant of the Adelaide geosyncline in the form of a trough filled with saline sediments (Tammemagi and Lilley (1973)). In a later paper Cleary, Simpson and Muirhead (1972) associated the conductivity anomaly with the western edge of their low velocity wedge (see above). It may be possible to distinguish between these alternative explanations of the conductor by recording a seismic profile across the region in which the anomaly occurs, using blasts at the Leigh Creek coalfield as sources of seismic energy, or by making detailed measurements of heat flow over the area.

This brief review of seismic, magnetic and geological studies makes it apparent that the Adelaide geosyncline must feature prominently in any account of the past and present tectonic processes occurring in the central southern Australian continent. Since seismic waves from earthquake sources have so far provided the most comprehensive information about these processes, it is desirable to have an accurate model for the variations of seismic wave velocities in the crust for the accurate location of earthquake hypocentres. The remaining chapters describe an attempt to determine such a model, and the model itself.

Figure 2.1 Map of South Australia showing locations of

(a) permanent seismic stations (Δ)

(b) blast sites used in this study (*)

(c) major seismic profiles (————)

(d) previous seismic experiments (+)

in relation to the Adelaide Geosyncline.

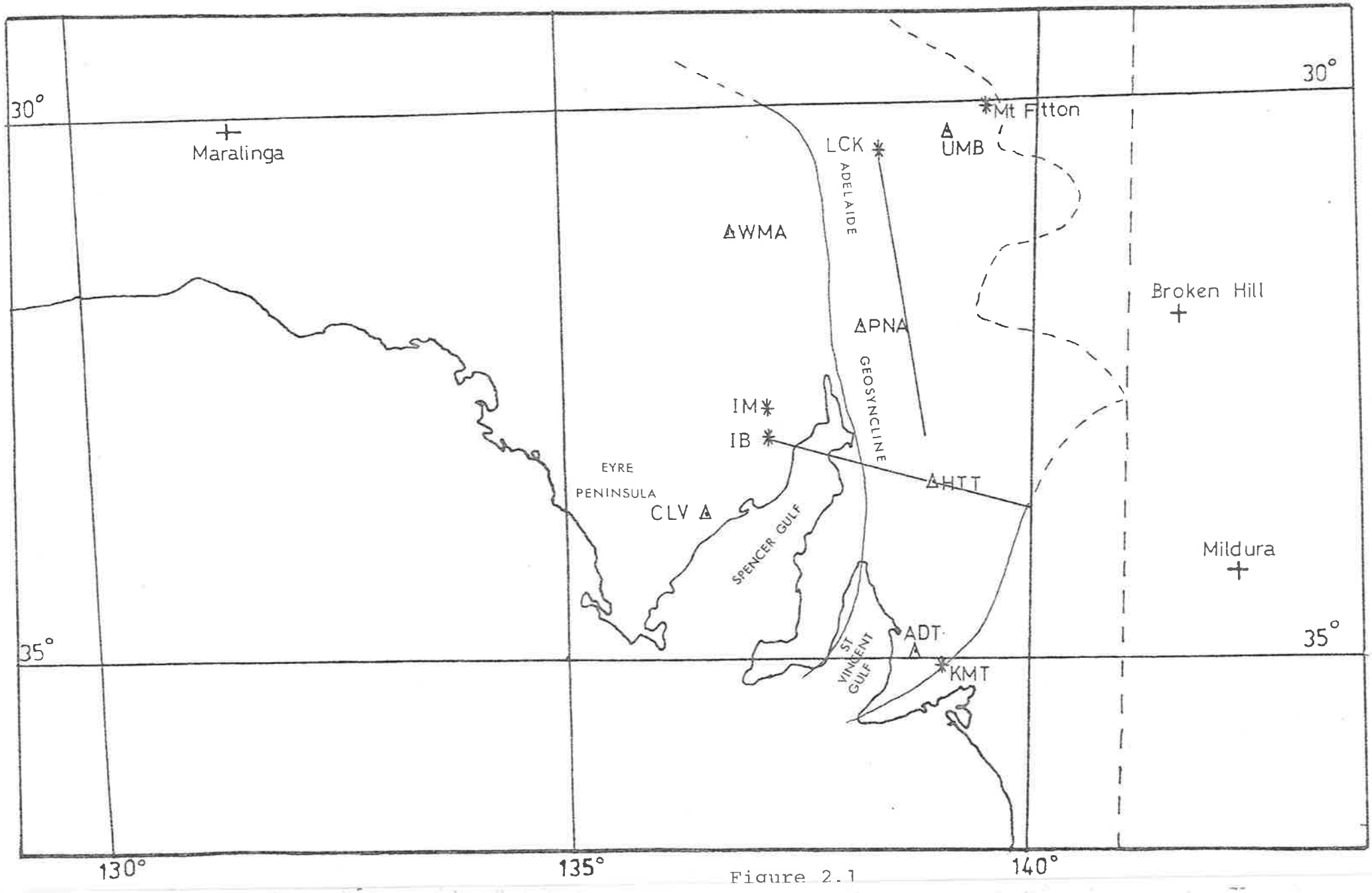
30°
30°
Maralinga
Mt Fitton
LCK
UMB
ADELAIDE
WMA
Broken Hill
PNA
GEOSYNCLINE
IM
IB
HTT
EYRE
PENINSULA
CLV
SPENCER GULF
Mildura
35°
35°
ADT
ST VINCENT GULF
KMT
130°
135°
140°

Figure 2.1

CHAPTER 2

EXPERIMENTAL PROCEDURE

2.1 The Profiles

Recording was attempted along three linear profiles, using as seismic sources the blasts at three large open cut mining operations. The directions of the profiles were south of the Leigh Creek (LCK) coal mine, east from the Iron Baron (IB) haematite mine, and north from the Kanmantoo (KMT) copper mine. This choice of profiles afforded the possibility of achieving a reversed profile along the axis of the geosyncline from Leigh Creek to Kanmantoo, and a single unreversed profile approximately perpendicular to the geosyncline axis. Unfortunately, the KMT mine ceased operation before the northerly set of recordings was completed. Following the recommendation of Landisman and Mueller (1966), who suggested that a station spacing of 5 km is suitable for reconnaissance work, and 500 m for precision measurements (!), a nominal spacing of 5 km between stations was adopted for the profiles, although this was not always realised. The 5 km spacing was considered to be reasonable in view of the large distances involved, and the limited time available for recording.

The locations of the quarries and the orientation of the profiles are shown in Figure 2.1.

In addition to the temporary recording stations which

PLATE I Kinemetrics PS-1A Recorder
and Mark Products Seismometer.

were established at new sites along the profiles for each blast, six of the permanent seismic stations of the University of Adelaide's recording network were sufficiently close to the quarries to be able to record most of the blast events. The sites of these permanent stations are also shown in Figure 2.1.

2.2 The Recording Equipment

Recording commenced in late 1974 with a single recording unit consisting of a Kinemetrics PS-1A drum recorder and 1 second period SS-1 seismometer. This was later supplemented by the addition of two identical units. The use of identical recording systems was considered to be desirable to facilitate correlation of phases along each profile. The Kinemetrics PS-1A drum recorder is a lightweight recorder built into an aluminium suitcase. The system consists of four main components.

(1) a low noise high gain seismometer amplifier with a pass band between 0.03 and 100 Hz,

(2) a Filter/Motor Drive Unit, which offers a selection of six different filters for filtering the signal before recording, a crystal oscillator clock supplying 1 minute and 1 hour timing pulses, a power amplifier to drive the drum recorder motor, and a Mixer where timing pulses and seismometer Amplifier output are added,

(3) a 110 mm diameter x 30 cm long drum with pen drive motor and stainless steel recording stylus and,

(4) a battery pack containing 4 x 6 volt rechargeable lead

PLATE II Sample Kinemetrics PS – 1A record written by sapphire stylus on smoked paper. Note the good resolution obtained.

Record was made at site L34 (see Figure 4.1) and shows seismic wave arrivals from blasts at IB, IM and KMT in addition to a teleseismic event (T).

The distance separating the two bands of time marks represents a 30 second interval.

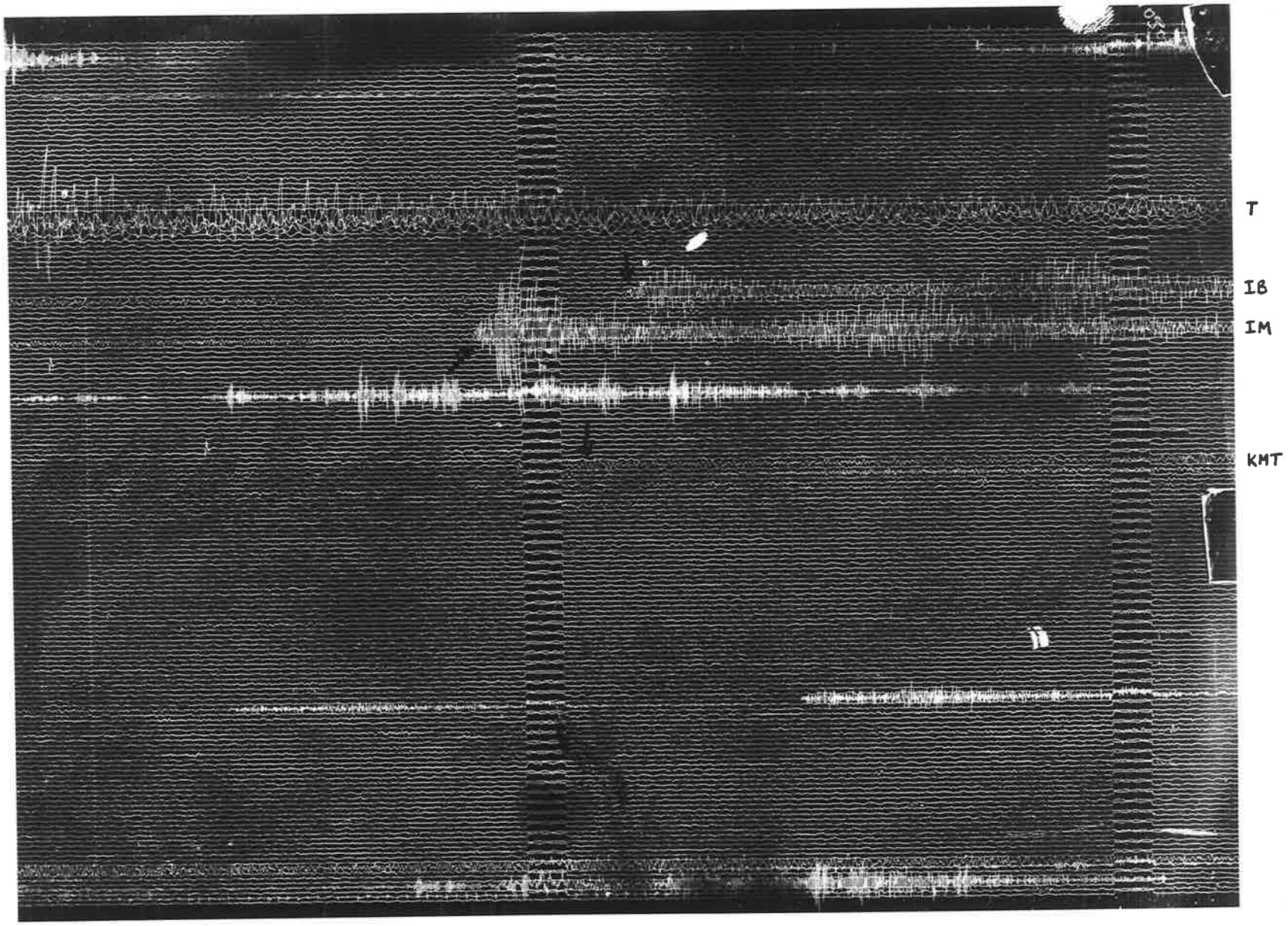
T
IB
IM
KMT

dioxide batteries which supply all the power required for system operation. Provision is also made to allow for the use of an external power source.

The PS-1A recorder is shown in Plate I, coupled to a Mark Products seismometer. In general the systems, as purchased, have been entirely satisfactory as portable, visual recorders, and required no modification for our purposes.

2.2.1 Recording medium

The records of the Kinemetrics PS-1A can be written by ink pen on paper or by sapphire stylus on smoked paper. The latter was found to afford better signal resolution at high frequencies, and was adopted for recording at all temporary stations for this reason. The quality of recording obtainable with this recording medium is evident from the sample record shown in Plate II. Further, it avoided two problems often encountered with capillary pens, viz. pen blockage and the pen's failure to write at high pen speeds. On the other hand the smoked chart required careful preparation, handling and fixing after recording. The procedure recommended by the manufacturer for fixing smoked charts involved the use of artist's spray fixative. This was found to be unsatisfactory in the field because of the toxic nature of the spray's fumes, and the tendency of the spray droplets to coalesce, so that the carbon surface became spotted by the impact of large spray drops. The method of dipping the charts into a dilute solution of shellac in methylated spirits was subsequently adopted for

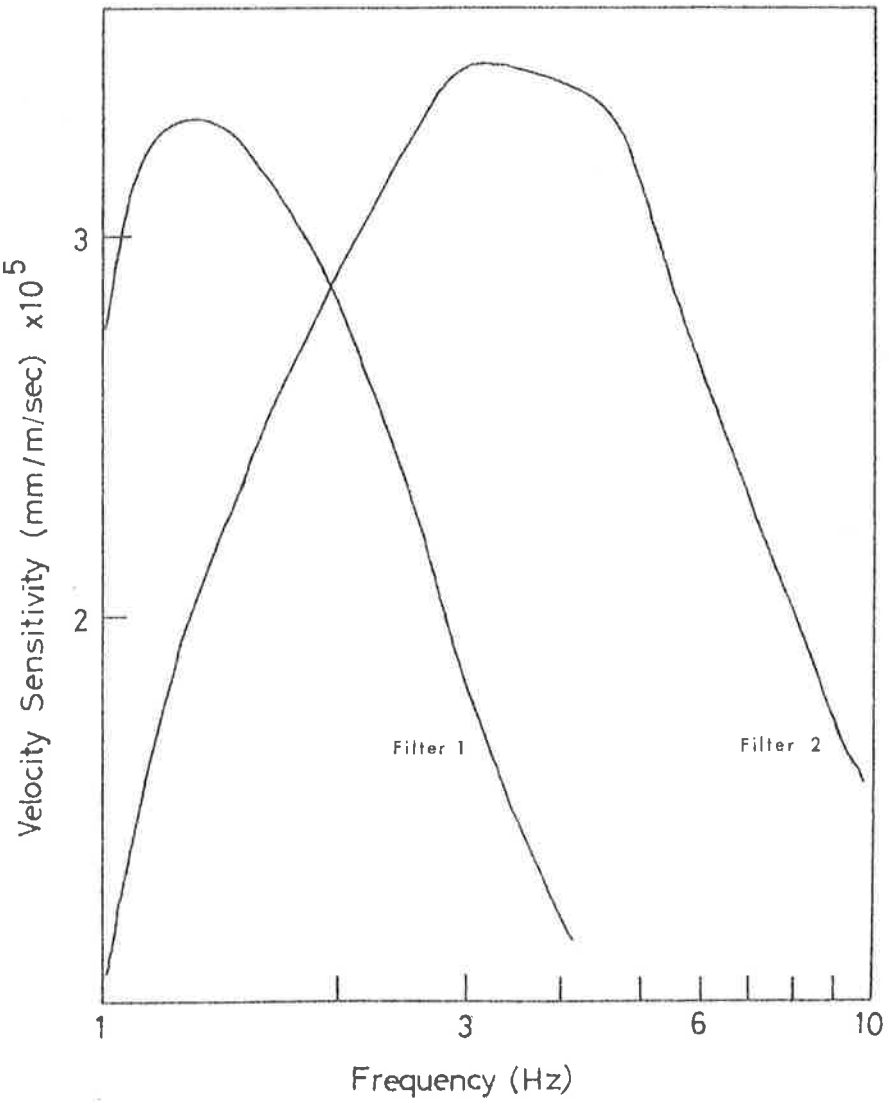

Figure 2.2

Frequency Response Curves of Recording System, for two Filters most suited to recording Quarry Blast Events.

Attenuation 50 dB.

fixing. Besides avoiding the problems of sprays mentioned above, shellac solution is considerably cheaper than the spray fixatives, and although discolouration of the paper leads to loss of contrast between the trace and the carbon coating, the loss is slight and the method is altogether preferred, particularly in the field.

2.2.2 Signal filtering

The typical frequency response of a Kinemetrics PS-1A/SS-1 recording system (seismometer plus recorder) is shown in Figure 2.2 for the filters numbered 1 and 2 for frequencies to 10 Hz, and amplifier attentuation of 50 dB.

Filter 2 was considered to be the most satisfactory filter setting, taking into consideration both the high frequency noise associated with wind and human activity, and the 1 second microseisms often associated with the movement of "cold fronts." In order to demonstrate the suitability of filter 2 for recording events at large distance from the source, where low frequencies would be expected to predominate in the signal, two events were recorded on instruments operating with different filter selections, at sites approximately 245 and 360 km from the IB source.

Although these "tests" were made late in the recording programme, the results supported the intuitive choice of filter 2 for recording at all distances. The record traces in Figure 2.3(a) illustrate this point. A recording using

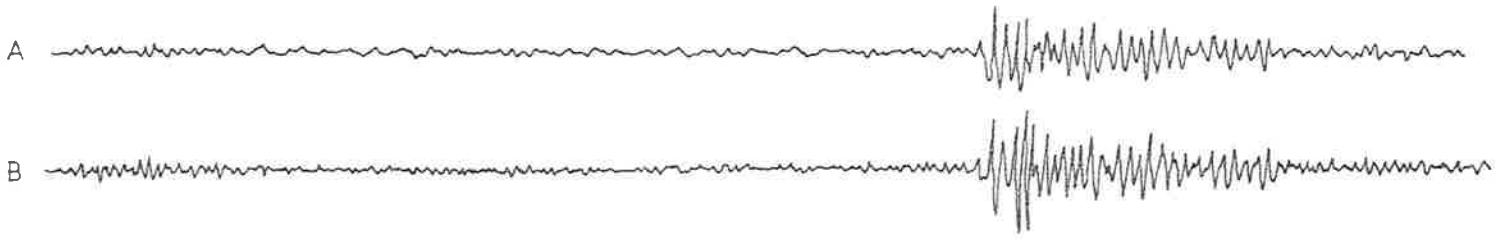

Figure 2. 3 (a) Records of IB blast, 19/4/75, obtained with filters #1 and #2

A. Filter #1, Attenuation 18 dB, Distance = 245 km

B. Filter #2, Attenuation 18 dB, Distance = 245 km

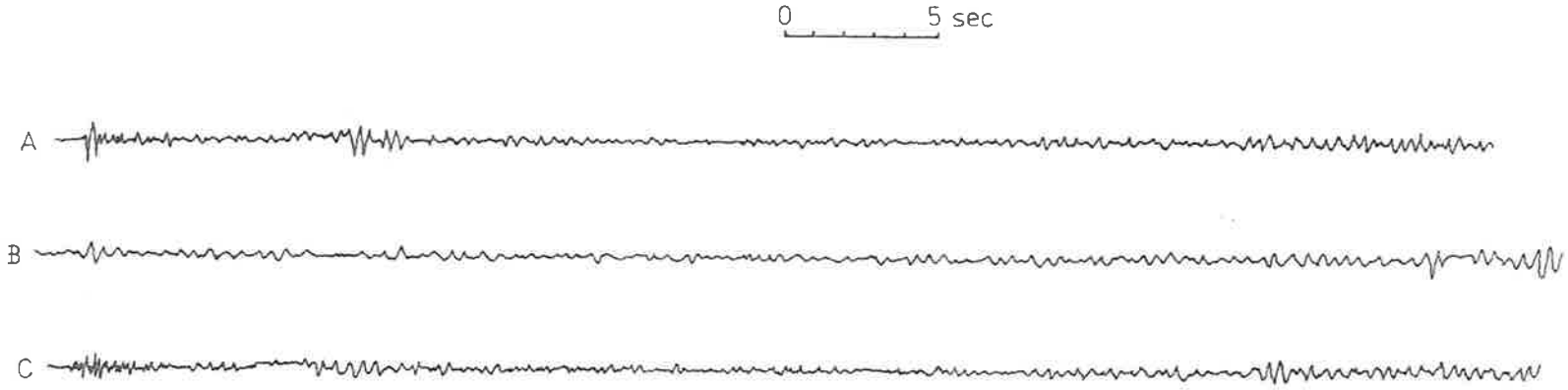

Figure 2. 3 (b) Records of IB blast, 26/10/76, with filters #1 and #2

A. Filter #2, Attenuation 30 dB, Distance = 355 km

B. Filter #1, Attenuation 30 dB, Distance = 360 km

C. Filter #2, Attenuation 30 dB, Distance =365 km

filter 4 on 19/4/75 showed no event corresponding to the arrivals on the two adjacent instruments using filters 2 and 1, possibly because of the high attenuation (30dB) needed to reduce the high frequency background noise which was caused by light wind gusts. For filters 1 and 2, however, the quality of recording can be seen to be comparable, if not better in the case of filter 2. The predominant frequency in the S-Wave portion of the wave train is about 3 Hz, for both records.

The second set of records (Figure 2.3(b)) from which a comparison can be made of recordings obtained with different filtering, was obtained at much greater distance from the source than the first set, and again, the results confirm the use of filter 2. The frequency in the S group of waves is slightly greater than 2 Hz for both records.

2.2.3 Other details

After November 1974, all recorders were operated with a paper speed of 4 mm/s, which gave a total recording time of 6 hours/chart. This length of recording time was well suited to quarry blast recording, since it allowed coverage of both morning and afternoon blast times, without the need to attend recorders being operated at remote sites.

Amplifier gains were generally attenuated by between 18 and 36 dB from maximum gain, with the limiting factor being the background noise level at any site.

Arrival times of recorded phases were read from hour and minute marks derived from the crystal clock in each recorder. These clocks were synchronized to the time signal broadcast on short wave bands at 4.5, 7.5 and 12 MHz from VNG, Lyndhurst, Victoria by the Australian Telecommunications Network. Time marks at 1 second intervals, derived directly from the radio time signal, were also applied to the beginning and end of most charts to allow clock corrections to be made.

2.3 Recording Sites

Recording sites were chosen to lie as near as possible to the profiles shown on Figure 2.1. Deviations from linearity were generally less than 5 km. Topographic maps of 1:250,000 scale prepared by the Department of Lands, South Australia, and the Royal Australian Survey Corps, were used to locate the recording sites in the field. These locations, together with field notes, were later used to relocate the recording sites on maps of scale 1:50,000, or, where these were not available, on 1 mile geological maps prepared by the South Australian Department of Mines. As a result, the coordinates of recording sites are known to within ± 100 m or better.

In addition to the constraints placed upon receiver locations by the very nature of a linear seismic profile, sites had to be readily accessible, yet remote from roads, railways, windmills, trees, and grazing livestock.

Seismometers were preferably sited on outcropping rocks, and covered with inverted bins to act as wind shields. In areas of alluvial cover, where this was not possible, the seismometers were placed in holes which were then covered with aluminium sheets and soil.

Although no formal attempt was made to investigate the effects of conditions at the seismometer sites on record quality, an appreciation of such effects has been gained from a simple study of 113 records which were obtained under a wide variety of recording conditions. The amplifier gain used for each record was noted and included in one of two groups according to the nature of the base material on which the seismometer was situated. The two simple categories used were (a) those sites at which the seismometer was placed in a hole dug in clay or sand, and (b) those sites at which the seismometer was placed on a solid rock base. In the first case, the depth to firm rock was not established at any of the sites, but it is estimated that in all cases rock was covered by at least several feet of alluvium, as judged from the surrounding soil conditions and lack of rock outcrops. It was found that for the 72 records included under category (a) above, the mean attenuation required for reducing background noise to an acceptable level was 26 ± 5.3 dB. For the 41 records included under category (b), the mean attenuation used was 21 ± 3.8 dB. This shows that on the average an increase of gain by 5 dB was possible for seismometers placed on rock, compared with those placed on alluvial material, for the same background noise level. The

attentuation values observed for the above two groups of records have large standard deviations which tend to obscure the real differences between the two types of sites. The large scatter in the values of attenuation for each group reflects the fact that no account was taken in the categorisation of the records, of different meteorological conditions which prevailed during the recording periods. In an attempt to isolate the effect of the soil conditions at the sites from other factors effecting useable gain a set of 12 records was selected from 6 occasions when two seismometers were operating on rock and soil bases respectively, albeit not at the same location. These records confirm the findings from the larger record collection. The differences of gain useable on rock/soil bases on any day were found to range from 6 to 12 dB, with the rock sites invariably being quieter. It should also be noted, however, that despite the lower amplifier gains of between two and four times for the system placed on soil, compared with that on rock, the event amplitudes were comparable, indicating that signal amplification had occurred when seismic waves emerged through low velocity alluvial cover. It was also observed, as might be expected, that disturbances due to vehicular and pedestrian traffic were generally less pronounced for seismometers placed on rock, than for those placed on soil bases.

A planned, formal study should be undertaken to define quantitatively, the various contributions to seismic noise level and the effect of site location and seismometer placement on site quietness. For detailed noise analyses,

broad band tape recording facilities would be essential, in addition to visible chart recorders.

2.4 The Seismic Sources

2.4.1 Leigh Creek Blasts

Blasts at three different sites provided the seismic energy for observations along the profile south of Leigh Creek (LCK-S). Two of the blast areas were in lobes D and C, which were approximately 4 km apart at the northern and southern ends of the Northfield coal basin respectively. The third blast area was located 8 km south of Leigh Creek township on the edge of the Telford basin, where a drainage channel was being prepared to divert surface water around the Telford basin, prior to the commencement of mining there. The blasts in lobes C and D were fired in Triassic shales, for the purpose of loosening overburden for subsequent removal by dragline; the blasts for the drainage channel were situated in the older shales of the Proterozoic Amberoona formation. Although the charge sizes were comparable, and blasting techniques were apparently the same for both the lobes C and D, and the drain blasts, the amplitudes of the records of the blasts at the monitoring stations were considerably greater for blasts within the coal basin, than for blasts outside it. It has also been observed that blasts from the two lobes in Northfield have characteristic signatures at the permanent recording stations, which enable the lobes to be identified from the seismic records. Charge sizes ranged from 566 to 1950 kg of

ammonium nitrate, and all shots were fired instantaneously by electrical detonation.

Although both lobes are quite extensive, blasts were confined to relatively small areas within each lobe during the period of recording, so that the centres of those smaller areas have been used for the determination of source-station distances. The coordinates of the centres are given in Table 2.1, where the error terms represent the maximum possible extent of movement of the blast site within each lobe. It can be seen that the extent of movement is greatest for lobe C, and in each case is greatest in the east-west direction. This means that source to station distances and travel times will be less affected by movement of the shot point for stations lying south of the source than for stations lying east or west. In particular, it means that the movement of the shot point will introduce errors into the data chiefly through its effect on the travel times to the monitoring stations WMA and UMB which lie approximately east and south-west of the blasts. The cumulative effect on travel times to permanent stations, of both movement of the shot point, and errors in reading the station records is indicated in the error terms quoted in Tables 3.1(a) and 3.1(b).

Table 2.1 Coordinates of LCK Blasts

Lobe	Latitude	Longitude
D	$30^{\circ}24.54'$ ± 60 m	$138^{\circ}23.84'$ ± 150 m
C	$30^{\circ}26.57'$ ± 400 m	$138^{\circ}24.29'$ ± 600 m
Drain	$30^{\circ}30.66'$ ± 100 m	$138^{\circ}25.35'$ ± 200 m

2.4.2 Iron Baron Blasts

Most of the records which were obtained along the profile east of Iron Baron (IB-E profile) were for blasts at the Iron Baron mine itself. A few additional records were obtained, however, from blasts at Iron Prince and Iron Monarch mines which lie approximately one and thirty kilometres north of Iron Baron respectively. In accordance with the purpose of the blasting at these quarries, which is to blast dense hematite ore and jaspillite from quarry benches, the shots, unlike those at LCK, always involved delayed firing. Total charge sizes ranged from one to thirty thousand kilograms of nitropril, with typical quantities being between four to six thousand kilograms. The shots were fired by lit fuses. The co-ordinates (Table 2.2) which were used to calculate quarry-station distances, refer to the centres of the areas being worked, during the period of recording.

Table 2.2 Coordinates of IB, IM, IP Blasts

Quarry	Latitude	Longitude
IB	$33^{o}0.40'$ ± 500 m	$137^{o}9.61'$ ± 150 m
IP	$32^{o}59.59'$ ± 250 m	$137^{o}9.39'$ ± 100 m
IM	$32^{o}44.70'$ ± 100 m	$137^{o}8.41'$ ± 100 m

It is clear from the error terms, which again define the maximum extent of lateral movement of the shot point in each quarry, that the travel times to CLV will have a greater variance than the travel times to HTT.

2.4.3 Kanmantoo Blasts

As was the case at the other mines, the explosive charges used at Kanmantoo consisted of ammonium nitrate prill and fuel oil, with cordtex fuses linking the drill holes in the charge pattern. Delays were used at KMT, in order to maximize the efficiency of the blast, and to reduce low frequency vibration at the nearby townships of Kanmantoo and Callington. The charges were detonated electrically. Charge sizes were typically of the order of 4 to 8 thousand kilograms of ammonium nitrate. The co-ordinates of the centre of the pit, from which station distances were calculated were $35^{o}5.54'$ ± 230 m South and $139^{o}0'$ ± 240 m East.

2.5 Blast Times

The shot instants for the quarry blasts used in the survey, were calculated from the seismic records of the blasts obtained at the permanent recording stations nearest each quarry (see Figure 2.1). The travel times of seismic waves from each quarry to its respective monitoring stations were determined by recording several shot instants at each quarry and the corresponding arrival times of seismic waves at the monitoring stations. This procedure is described in Section 3.1.1. These travel times and the arrival times of seismic waves at each monitoring station from subsequent blasts, enabled the times of later blasts to be determined with an accuracy of ± 0.1 s. The stations used to monitor

each quarry's blasts were

Quarry	Monitor station
Leigh Creek (LCK)	Umberatana (UMB)
	Woomera (WMA)
	Partacoona (PNA)
Iron Baron (IB)	Hallett (HTT)
Iron Monarch (IM)	Cleve (CLV)
	Partacoona
Kanmantoo (KMT)	Adelaide (ADE)
	Hallett

In determining the origin time of a particular blast, greatest weight was given to the time obtained from the records at the first station in each of the above groups, the others being used primarily as checks. The details of the quarry-station travel time determinations are included in the following chapter.

CHAPTER 3

TRAVEL TIMES TO STATIONS OF THE PERMANENT SEISMIC NETWORK AND THEIR IMPLICATIONS FOR CRUSTAL MODELS

3.1 Travel Times to Stations of the Permanent Seismic Network

Throughout the period of the present study, six of the permanent seismic stations operated by the University of Adelaide continued to record events from the quarries shown in Figure 2.1. In this chapter the travel times from the quarries to the permanent stations are discussed.

3.1.1 "Calibration" Blasts

The travel times of seismic waves from each quarry to its respective monitoring station(s) were obtained from the direct measurement of shot instants for a number of blasts at each quarry, and the corresponding arrival times of seismic waves at the nearest stations to each blast.

The shot instants of the "calibration" blasts were initially recorded on a Both strip chart recorder, coupled to a prospecting geophone which was placed as near as possible to the blasting area (usually within 200 m.). One second time marks derived from the VNG radio time service were also recorded directly onto the chart. This rather cumbersome system with its temperamental ink pens and time channel relays was later replaced by a simple cassette

recorder adapted to record both event and radio time pips directly onto magnetic tape for subsequent play back in the laboratory. The Both paper speed of 1.7 cm/s and the cassette playback via a Schlumberger ultraviolet recorder with a chart speed of 2.5 cm/s meant that shot times could be measured to ± 0.02 sec with either recording system. The results of these "calibration" blasts are given in Table 3.1 (a) and (b).

Table 3.1 (a) Travel Times to Permanent Stations nearest to each Blast; from "Calibration" Blasts

QUARRY	STATION	NUMBER OF BLASTS	DISTANCE (km)	TRAVEL TIME (SEC)
LCK	UMB	4	72.65	12.01 ± 0.01
IB	CLV	4	97.81	16.16 ± 0.05
	HTT	4	170.68	28.05 ± 0.06
IM	CLV	1	120.60	19.98
	HTT	1	182.72	29.55
KMT	ADT	3	29.55	5.35 ± 0.05

Table 3.1 (b) Travel Times to Distant Permanent Stations; from "Calibration" Blasts

QUARRY	STATION	DISTANCE (km)	TRAVEL TIME (SEC)
LCK	PNA	178.25	30.07 ± 0.06
	WMA	172.72	28.93 ± 0.04
IB	PNA	145.59	24.65 ± 0.10
	WMA	209.03	33.5 ± 0.06
KMT	HTT	184.35	30.54

3.1.2 Routine Blasts - a Check on the Travel Times

In addition to the "calibration" blasts of the previous section, many more blasts at each quarry were recorded at the permanent stations. Although no absolute origin times were measured for these blasts, differences of travel times of seismic waves to any pair of stations, can be simply found by subtracting the arrival times at the two stations, of waves from a particular blast. Table 3.2 contains the mean differences of travel times for several pairs of stations, for each blast source. The standard deviation of the mean has been given for each of the mean travel time differences and can be accounted for by errors in reading onset times of arrivals and by movement of the shot points in the quarries.

Table 3.2 Differences of Travel Times to Pairs of Stations, for Routinely Recorded Blasts

QUARRY	STATION PAIR	NUMBER OF EVENTS RECORDED	MEAN TRAVEL TIME DIFFERENCE (SEC)
LCK	UMB-WMA	9	16.93 ± 0.03
	UMB-PNA	7	18.06 ± 0.03
	PNA-WMA	8	1.12 ± 0.03
IB	CLV-HTT	20	11.87 ± 0.03
	CLV-PNA	15	8.47 ± 0.05
	CLV-WMA	15	17.34 ± 0.06
KMT	HTT-ADE	10	25.16 ± 0.05
IM	HTT-CLV	12	9.68 ± 0.03

It can be seen that the differences of arrival times at pairs of stations (Table 3.2) agree very well with the corresponding differences which can be calculated from the "calibration" travel times (Tables 3.1 (a) and (b). This agreement is significant because it (a) indicates the stability in time of the quarry-to-station travel times, and (b) confirms the observer's ability to read the permanent station records consistently. These two factors are crucial for the method of obtaining the times of blasts from the permanent station records, as described in Section 2.5. Values for the differences between travel times to pairs of stations from major quarries have also been used in the identification of quarry blast records, and in particular they have been used to distinguish quarry blasts from local earthquakes on the records of the permanent seismic network.

In addition to serving the above purposes, differences of arrival times at pairs of stations have enabled travel times to distant stations which did not record the calibration blasts, to be determined from the records of subsequent blasts. These additional travel times, which are not included in Tables 3.1 (a), (b), are listed in Table 3.3.

3.1.3 Travel Times from Mt Fitton

An additional set of travel times to the permanent recording stations has been obtained from a large explosion detonated at the Mt Fitton copper mine in the northern Flinders Ranges. The travel times from this blast were

analysed by Finlayson et al (1974), who studied travel times to the north and west of the blast, and by Muirhead et al (1977) who made observations to the east. Both reports included the travel times to the six South Australian permanent stations.

Table 3.3 Travel Times to Stations which did not Record "Calibration" Blasts, Including Travel Times from Mt Fitton Blast

QUARRY	STATION	DISTANCE (km)	TRAVEL TIME (SEC)
LCK	CLV	405.44	58.28
	HTT	338.39	50.62
IB	UMB	358.78	52.79
	ADE	260.33	41.60
IM	PNA	126.60	21.2
	WMA	180.28	29.32
Mt Fitton	UMB	49.21	7.98
	PNA	258.52	39.15
	ILN	300.3	44.57
	HTT	384.14	54.97
	CLV	500.68	68.22
	ADT	555.36	76.31

Two interesting observations were made about the S.A. travel times by the two groups of workers. Finlayson et al observed that there existed a "large degree of scatter {for the travel times to the South Australian stations} which was not apparent in the Maralinga times of Doyle and Everingham". Muirhead et al found that the times to the South Australian

Figure 3.1 Reduced travel time graph for first arrivals at stations of the permanent seismic network, from various blast sources.

The blast - station pair is shown for each of the data points.

The broken lines are the travel time curves for Pl and Pn arrivals of the Doyle and Everingham (1964) study.

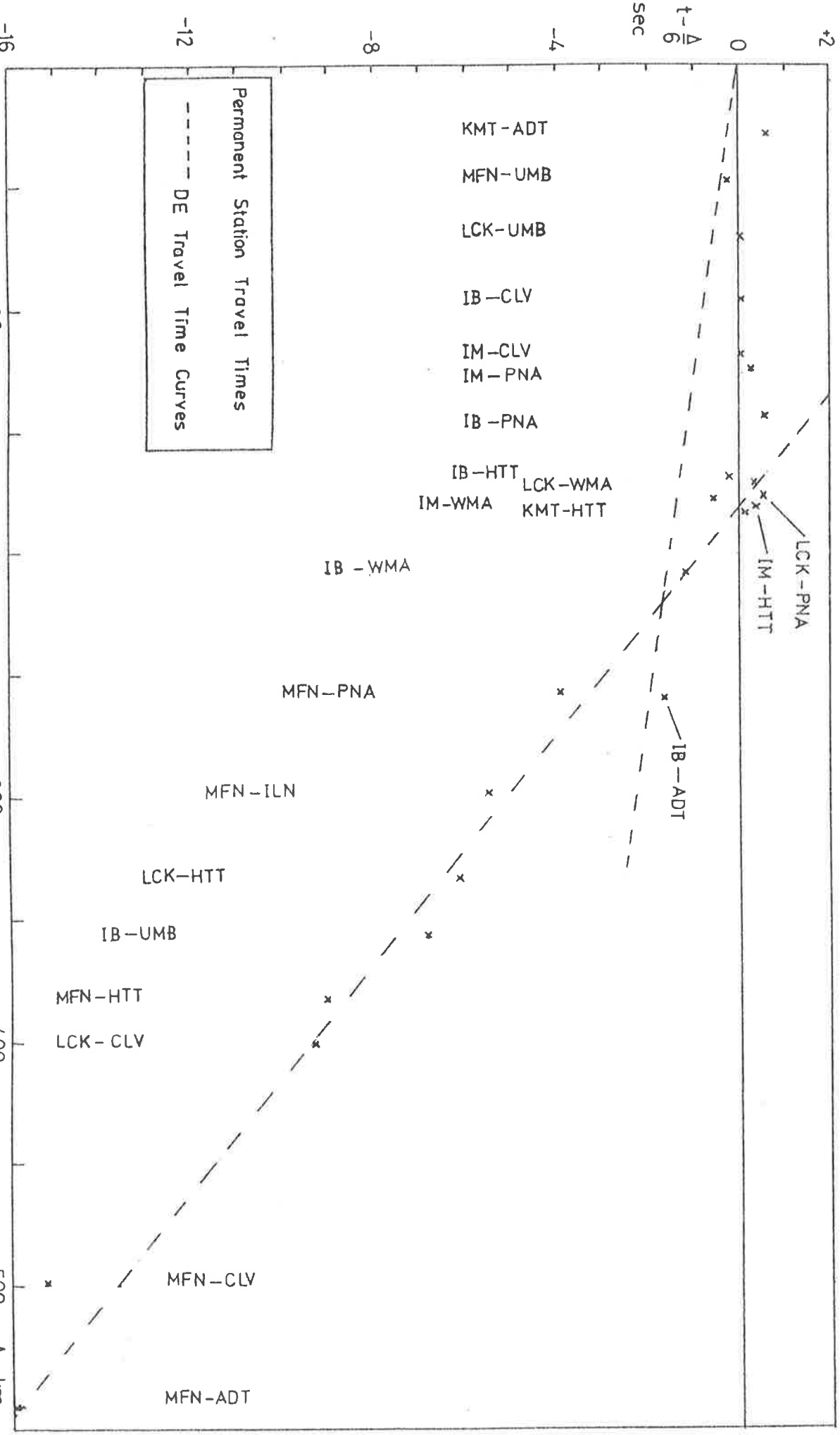
Permanent Station Travel Times
DE Travel Time Curves
t-Δ/6 sec
-16
-12
-8
-4
0
+2
100
200
300
400
500
Δ km
KMT-ADT
MFN-UMB
LCK-UMB
IB-CLV
IM-CLV
IM-PNA
IB-PNA
IB-HTT
LCK-WMA
IM-WMA
KMT-HTT
IB-WMA
MFN-PNA
MFN-ILN
LCK-HTT
IB-UMB
MFN-HTT
LCK-CLV
MFN-CLV
MFN-ADT
LCK-PNA
IM-HTT
IB-ADT

Fig. 3.1

stations from Mr Fitton had "marked delays" relative to the travel time branch defined by arrivals at portable stations operated by the Australian National University further east (see their Fig. 5). When the South Australian records were re-read by independent observers, however, and travel times calculated using the origin time of the Mt Fitton blast given by Finlayson et al, then the arrivals were found to be consistent with the easterly observations. These times are included in Table 3.3.

3.2 Crustal Models

The travel times obtained from quarry blasts in the present study offer an alternative to the data from earthquakes used previously by Stewart and White, for the determination of crustal structure in South Australia. Since both sets of travel times have been observed by essentially the same seismic network, it is of interest to compare the crustal models which the earthquake and quarry blast data satisfy.

3.2.1 Model from First Arrivals

In Figure 3.1, the data of Tables 3.1 (a), (b),&3.3 are plotted on a reduced time axis, with a reducing velocity of 6 km/s. The data points lie approximately on two straight line segments. The simplest crustal model that is consistent with the first arrivals is that consisting of a homogeneous crustal layer overlying an infinite half-space,

the mantle. The crust-mantle boundary is assumed to be horizontal over the region encompassed by the network of recording stations and sources. The first arrivals seem to divide into two sets according to distance from the source. These are:

(a) the first arrivals recorded at distances of less than 150 km which have an apparent velocity of approximately 6 km/s. These arrivals are taken to be the direct wave (P1) arrivals.

(b) the first arrival times at distances greater than 150 km define a travel time branch with an apparent velocity which is commonly associated with ray paths which have been critically refracted at the Moho. This is the interpretation given to these arrivals. The apparent velocities and estimated depths to the Moho are given in Table 3.4.

Table 3.4 Upper Mantle Velocities and Moho Depths Derived from the Permanent Station Data

DATA USED	APPARENT VELOCITY km/s	INTERCEPT (s)	M DEPTH (km)
Mt Fitton	8.00 ± 0.03	6.9 ± 0.18	31.2
LCK & IB	8.05 ± 0.05	7.6 ± 0.27	34.2
all data for Δ>150 km	8.08 ± 0.05	7.65 ± 0.29	34.3

Discussion: With the exception of events recorded at PNA, the ray paths corresponding to the P1 arrivals have been confined to areas where the depth to magnetic basement ranges up to 1500 m. (ref. Contour Map of Depth to Magnetic

Basement, S.A. Dept. of Mines) which suggests that the apparent velocity for these arrivals may be ascribed to the top of the Precambrian crystalline basement (see Section 4.2.a (b) for more detailed comments). The travel times are significantly greater, however, than those observed by Doyle and Everingham (1964) (see Figure 3.1) at similar distances on the Gawler Platform, and the apparent velocity is correspondingly lower than the Pl velocity of 6.3 km/s found by Doyle and Everingham, or that found by White or Stewart. The Pn travel time equation for events at LCK and IB agrees well with those found previously, both in terms of the apparent velocity of the Pn arrivals and the constant terms of the equations. The estimates of crustal thickness given in Table 3.4 are lower than those found previously because of the smaller value which has been adopted for the crustal velocity, on the basis of the Pl first arrivals. An increase of velocity with depth would be required to give a greater estimate of the depth to the Moho.

It should also be noted that the Pn first arrivals from Mt Fitton have an apparent velocity which is consistent with previously determined values, but that the constant term in the equation for the arrivals from this blast is anomalously low. The travel times from Mt Fitton are revised values which have been confirmed by three independent observers. An attempt to explain the early arrivals will be offered below. It is well known that the travel time equation for a refraction branch can be written as

$$T = \Delta/V + a_s + b_i$$

where a_s represents the source time term and b_i the i^{th} station time term (Willmore and Bancroft (1961)). The constant term in the linear equation fitted to the Pn arrivals is therefore equal to the sum of the station and source time terms, and any anomaly in the constant term can be attributed to an anomaly in one or other, or both of the time terms. From the LCK and IB data described above, and from additional data given in Chapter 4, the mean intercept term for Pn arrivals in South Australia is 7.7 ± 0.25 sec. This mean intercept has been determined from a large number of Pn arrivals which have been recorded over a wide range of azimuths, both at the permanent recording stations and at portable stations deployed throughout the geosyncline region. It therefore seems likely that the low intercept term obtained for the Mt Fitton arrivals is due to a low source time term rather than to anomalous station terms. This may indicate two things about the source region, (1) either the depth to the refractor is smaller than expected at the point at which the seismic rays become critically refracted at the Moho or (2) the crustal velocity is higher than expected in the region surrounding the source, or there may be a combination of these factors operating. If the reduction of source term for Mt Fitton is 0.7 sec compared to the LCK and IB source terms (from Table 3.4), then the high crustal velocity hypothesis requires a velocity of 6.4 km/s for the Pl velocity in a homogenous crust of thickness 34 km, while the shallow Moho hypothesis requires a crustal thickness of 28.6 km for a crust having a Pl velocity of 6 km/s.

It is of interest to note that the Mt Fitton mine is situated in a region of positive Bouguer gravity values, which approximately coincides with the long arcuate zone of high electrical conductivity reported by Gough et al (1974) (see also Section 1.3 above). It is possible to speculate that upwelling mantle material is responsible for three observations viz. the low source time term for the Mt Fitton blast, the positive gravity anomaly and the electrical conductivity anomaly. Preliminary calculations of the expected gravity anomaly that would be produced by mantle material welling up into the crust, as suggested by the seismic results from Mt Fitton, have shown that the observed gravity anomalies are too small to be attributed to upwelling mantle on the scale required for the seismic results. A seismic profile using LCK blasts as sources and directed towards Mt Fitton could be used to investigate structure on the Moho in the region about Mt Fitton.

A third explanation of the early arrivals at the South Australian stations from the Mt Fitton blast is that the shot time for the blast is in error. If the blast time were 0.7 sec earlier than the time quoted by Finlayson et al, then the Mt Fitton travel times would be consistent with other observations made in South Australia, and there would be no need to reduce the Bass Straight times by 0.8 sec, in order to "normalize" them to the Mt Fitton travel times (see Muirhead et al).

3.2.2 Model from S - P Intervals

An attempt was made to determine a uniform crustal model, consistent with the travel times to the permanent stations, using the method employed by White (1969) for earthquake data. White's approach would seem to be very useful when earthquake data alone were available, since precisely located epicentres are not required for the analysis. The method uses the relationship between (t_s-t_p) and t_p where (t_s-t_p) represents the travel time difference between any pair of critically refracted S and P wave arrivals, not necessarily from the same refractor, and t_p is the corresponding P travel time. The equation relating these variables is

$$(t_s-t_p)=t_p\ (\frac{v_p}{v_s} - 1) + (I_s - I_p \cdot \frac{v_p}{v_s})$$

where v_p and v_s are the P and S wave apparent velocities and I_s and I_p are the intercepts of the critical refraction branches for S and P arrivals respectively.

If values of (t_s-t_p) are plotted against t_p for all combinations of S and P arrivals, from all refractors which are present, then the slopes of the line segments determine the corresponding v_p/v_s velocity ratios, and the assumption of one velocity determines the remaining crustal parameters. The above procedure, applied to the permanent station records of quarry blasts, yielded conclusive results for P1 and S1 phases only. Data from station-quarry combinations where first P and S arrivals were unambiguously identified as P1 and S1 are plotted in Figure 3.2 and gave a velocity ratio

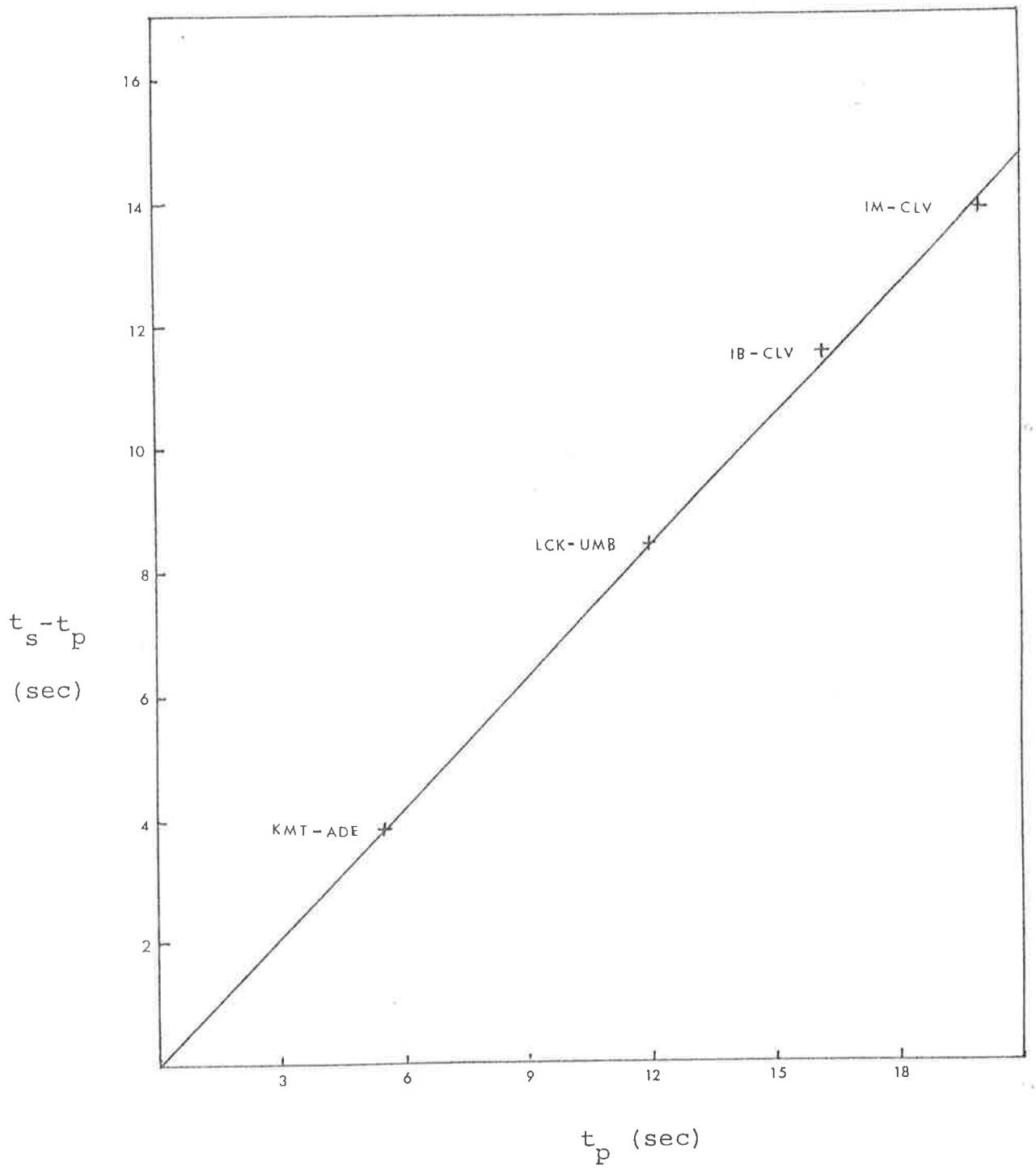

Figure 3.2 Plot of t_s-t_p vs t_p for P1 and S1 arrivals at permanent stations.

$$\frac{v_{p_1}}{v_{s_1}} = 1.69 \pm 0.01$$

which is slightly lower than the value of 1.74 determined by White from earthquake data, and Doyle and Everingham from Maralinga.

Data relating to phases other than Pl and Sl were few at distance ranges which may otherwise have provided unambiguous S-P intervals, particularly involving Pn. The available data do, however, indicate a greater crustal complexity than has previously been accepted for the South Australian crust. The inclusion of an intermediate refracting discontinuity in the crust results in a better explanation of the data than does a single layered crust, but even with this additional feature which, of course, generates more phases than a single layered crust, additional complexity seems to be required. A complicating feature of the method is the need to record accurate arrival times of shear phases.

3.2.3 Conclusions

The records of quarry blasts obtained at the permanent seismic network confirm the velocity of seismic waves in the upper mantle of South Australia of about 8 km/s, determined in several previous studies. The upper crustal velocity of 6 km/s however, is lower than that determined previously. This lower velocity of Pl waves may have significant implications for the location of earthquake hypocentres which

have previously been located in a uniform, single layered crust of Pl velocity 6.25 km/s. An attempt to account for both P and S wave travel times in terms of a simple, single layered homogeneous crust failed, partly because of inadequate data and partly because the available data reveal a greater complexity than would be expected for such a simple model.

An electrical conductivity anomaly discovered by Gough et al (1974) in the north eastern Flinders Ranges, may be related to an apparently anomalous source time term for the Mt Fitton blast, which was located in the region containing the conductivity anomaly, but the source of each anomaly and their possible relationship remains undetermined.

3.3 Teleseismic Residuals at the Permanent Stations

In addition to the travel times of seismic waves which have travelled relatively small distances through the earth's crust, the travel times of waves from teleseismic events may be used to provide information on crustal and upper mantle structural anomalies. If teleseismic residuals are compared at several stations which have small separations relative to their distances from the source, then it can be argued that anomalies or trends in the pattern of teleseismic residuals reflect anomalies or trends in the crust or upper mantle in the neighbourhood of the station(s), since the waves travel essentially the same paths through the mantle.

Accordingly, a small study was commenced to evaluate

the potential of the use of teleseismic arrivals for the study of the crust and upper mantle in South Australia. During January 1976 a number of earthquakes occurred in the vicinity of the Kermadec Islands at an epicentral distance of approximately 37^{o} from the South Australian seismic network. Twenty five earthquakes from this region were used to determine travel time residuals for each permanent station which may be interpreted in terms of anomalies in the velocity structure of the crust and upper mantle in the neighbourhood of each station. The earthquake epicentres were obtained from the Provisional Determinations of Epicentres published by USCGS, and travel time residuals were calculated from the travel time tables of Herrin et al (1968). In order to minimize the influence of errors in the source parameters, the residuals for each station were calculated relative to the residual at PNA. The station PNA was chosen as the reference station because of its centrality in the network. The results obtained from the Kermadec earthquakes are given in Table 3.5, together with the station corrections determined by Herrin and Taggart (1968) Cleary (1967) and Stewart (1972). It needs to be emphasized that the station terms quoted from the present study are relative terms only. The standard errors of the relative residuals are of the order of 0.15 sec. Faults which developed in the equipment at HTT and WMA and remained for much of the recording period, meant that only a very few useful earthquakes were recorded at these stations. The station terms for HTT and WMA are therefore bracketed to indicate the small sample size on which the two values are

based, and the consequent possible unreliablility of the values. A second set of teleseismic arrivals which was recorded by the network during the same period, from earthquakes at azimuths of between 300 and 350 degrees relative to PNA, confirmed the pattern of the station terms derived from the Kermadec earthquakes. In particular the large negative station terms at CLV and HTT were confirmed.

Table 3.5 Station Terms for Teleseismic Events

STATION	STATION CORRECTIONS (SEC)			
	HERRIN AND TAGGART	CLEARY	STEWART	PRESENT STUDY
UMB	-			0.09
CLV	-	-1.04	-0.08	-0.94
ADE	-0.4	-0.12	0.26	-0.30
HTT	-	-0.13	-0.18	(-0.91)
WMA	-			(-0.44)

Now the first arrival at CLV, from the blast at Mt Fitton (see Section 3.1.3) had a residual of -1.05 sec relative to PNA, and the first arrivals at CLV from blasts at LCK had residuals of approximately -0.5 sec from the travel time equation for Pn arrivals in South Australia (see Section 5.2.3). The blasts at Mt Fitton and LCK were at distances of 501 and 404 km respectively from CLV. Because approximately equal, large negative residuals are observed at CLV from events as close as 5^{o} and as distant as 37^{o}, it is almost certain that the low residuals are

produced by an anomaly in the velocity structure in the vicinity of the station. Negative residuals can be simply explained in terms of either higher velocities in the crust or mantle than expected, or, for Pn arrivals, a shallower refractor than expected. If the Mt Fitton and teleseismic residuals are produced by the same structural effect, then the residuals are most probably due to unusually high velocity material embedded in the upper mantle.

Although it has not been possible to make a definitive statement on crustal or upper mantle structure from this almost inadequate study of teleseismic residuals, the study has confirmed an early result of Cleary which was apparently contradicted by Stewart, in relation to the station residual term at Cleve. In so doing, the study has also shown that marked anomalies exist in station residual terms across South Australia, and that these are probably due to upper mantle effects. The vast amount of teleseismic data accrued by the permanent recording network could be used to study the likely sources of these anomalies.

CHAPTER 4

INTERPRETATION AND DISCUSSION OF SEISMIC PHASES RECORDED ON THE TEMPORARY STATION NETWORK - A CRUSTAL MODEL DEFINED

4.1 The Approach to Data Analysis and Interpretation

The bulk of the data used in the present study were obtained along two linear, unreversed refraction profiles which were approximately mutually perpendicular. A third partly completed profile provided some additional data. This chapter contains a discussion of the seismic phases observed on the three profiles and the apparent travel time equations by which they can be described.

The approach to the travel time inversion problem was to fit either linear or hyperbolic travel time equations to groups of arrivals which had continuity across several records. In the case of phases to which hyperbolic equations were fitted, the arrivals had curved travel time segments, large amplitudes and high apparent velocities characteristic of reflected arrivals (Cerveny (1966)). From the travel time equations, which were fitted to the data by the method of least squares, a simplified model of the crust was obtained, assuming uniform, horizontal layering of the crust. The basic crustal model so obtained was then subjected to various "perturbations" to produce more complex models incorporating positive and negative velocity gradients and low velocity layers. For each model generated, theoretical travel times were calculated and compared with

observed times with the object of improving agreement between the two and also, by referring to all available phases, of producing an internally consistent crustal model. Thus no claims for uniqueness are made for the model, but only consistency with the observed data. Theoretical travel times were calculated using the methods of geometrical ray theory; a discussion of the limitations of geometrical ray theory and of alternative inversion schemes is given in Appendix A.

With respect to obtaining information from the seismic records, the problems of selecting phases and reading arrival times particularly of later arrivals, and the subjective practice of associating phases from several records with one another and with a particular travel time branch, were greatly alleviated by the preparation of record sections for each profile. Another problem was that recognised by Jeffreys (1962) who remarked upon the possibility of measuring so many phases on a seismic record that "whatever hypothesis might be under discussion, some reading would be found to agree with it". He suggested three criteria to test whether a movement is a newly arrived phase. They are a sharp increase in amplitude, a sudden change of period, and a sharp change of direction of movement of the trace. In this study an attempt was made to select arrivals according to the first of these criteria only, so that it is possible that phases with small amplitudes may have been overlooked.

4.2 Travel Times of P-Waves - LCK-S, IB-E and KMT Profiles

In discussing the travel times of seismic waves and the crustal models derived from these data, the following notation will be used to refer to the observed seismic phases: P1 (S1), refraction from the upper crust; P2 (S2), refraction from a lower crustal layer; Pn (Sn), refraction from the Moho. An R following these symbols will denote a reflection from the top of the corresponding layer.

Record sections were constructed for each profile, to aid in the identification of phases which were able to be correlated across several adjacent records. The "continuity" of phases has been one of the criteria used in the selection of phases to be read from the records. First arrivals are generally unambiguous, and have been read with a reading microscope and vernier. Although the onsets of second arrivals are more difficult to pick than first arrivals, the identification of later arrivals in this study has been made on the basis of sudden amplitude increases, so that the arrival times of late arrivals are known within ± 0.1 sec. There is also the possibility, however, that some small amplitude second arrivals have remained unidentified. The arrival time of each phase used has been read several times, thus confirming at least the author's consistency in choosing onset times, and at best indicating the accuracy with which arrival times are known. It is estimated that first arrival times are generally known within ± 0.03 sec, and that the arrival times of later arrivals have a maximum error of 0.1 sec. When errors in the determination of the

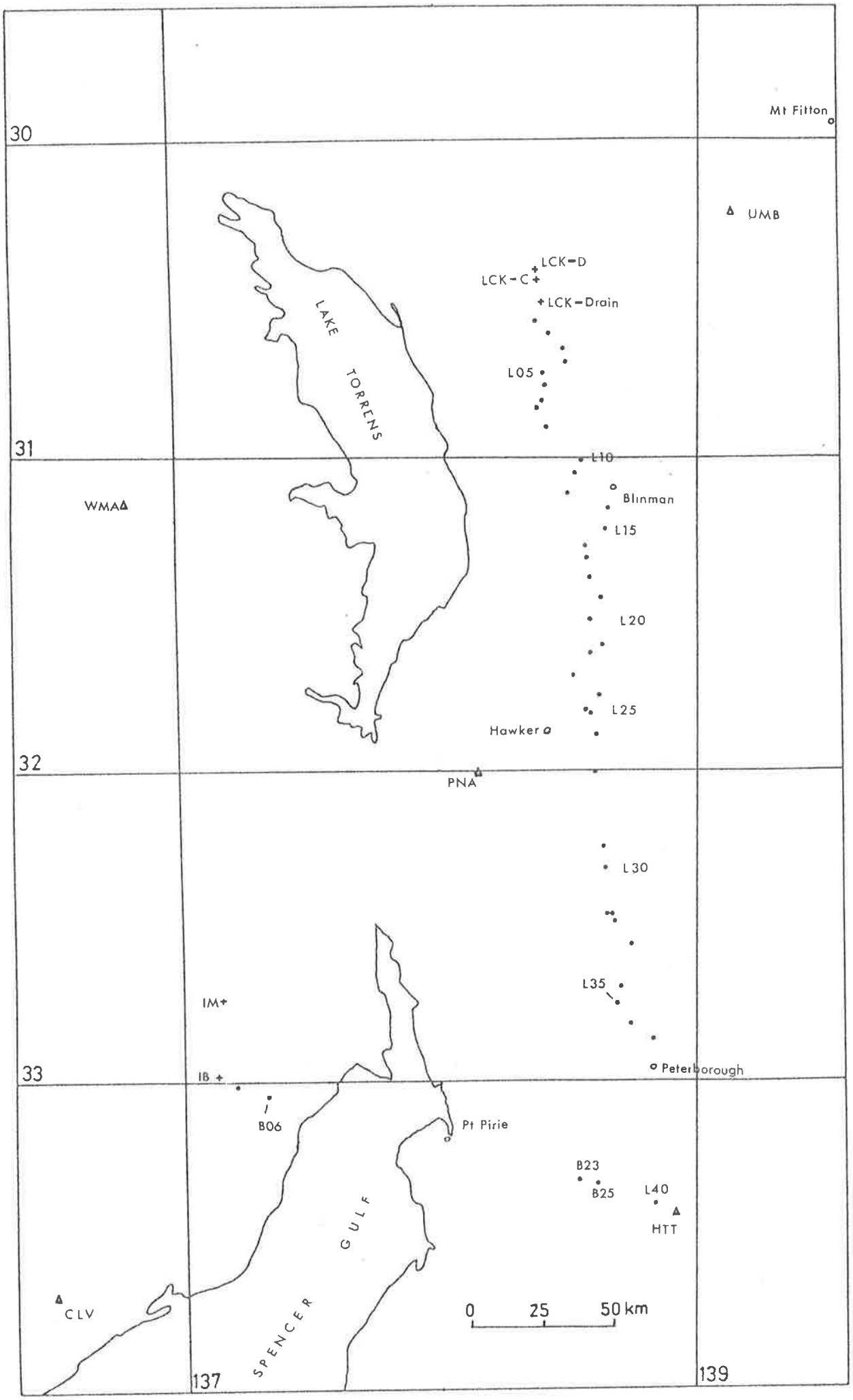

Fig. 4.1 Distribution of stations recording arrivals from blasts at LCK.

origin times of the blasts, which depend on the accuracy of reading permanent station records are taken into account, together with movement of the shot point, the errors in travel times are estimated to be less than 0.1 and 0.17 sec for first and later arrivals respectively. All travel times discussed below are listed in Appendix B.

4.2.1 Leigh Creek Profile

Forty two records were obtained along a profile (LCK-S) extending to 331 km from the source. An average spacing of 6 km between stations was achieved for stations to 180 km from the source, and 10 km was the average distance between stations at greater distances. The distribution of all stations which recorded arrivals from LCK blasts is shown in Figure 4.1. A reduced travel time graph of the P data plotted with a reducing velocity of 6 km/s is presented as Figure 4.2, in which it can be seen that all records at distances of less than 70 km from the source were of blasts at the drain site (see Section 2.4), that all except two of the records obtained beyond 200 km were from lobe C, and that most of the records in the intermediate distance range were of blasts at lobe D. The significance of this observation is that phases can be seen to be continuous on the record section, despite movement of the shot point by several kilometres. The stability of seismic phases in this sense, has long been employed as a test of their reality. In particular, the phase P2R which is interpreted as a reflected phase (see below) exhibits this stability.

Figure 4.2 Reduced travel time graph for seismic phases observed on LCK-S profile. Best fit curves have been superimposed (Equations 1-5 in Table 4.1).
Letter Code Dr, D, C indicates Drain, lobe D or lobe C source respectively.

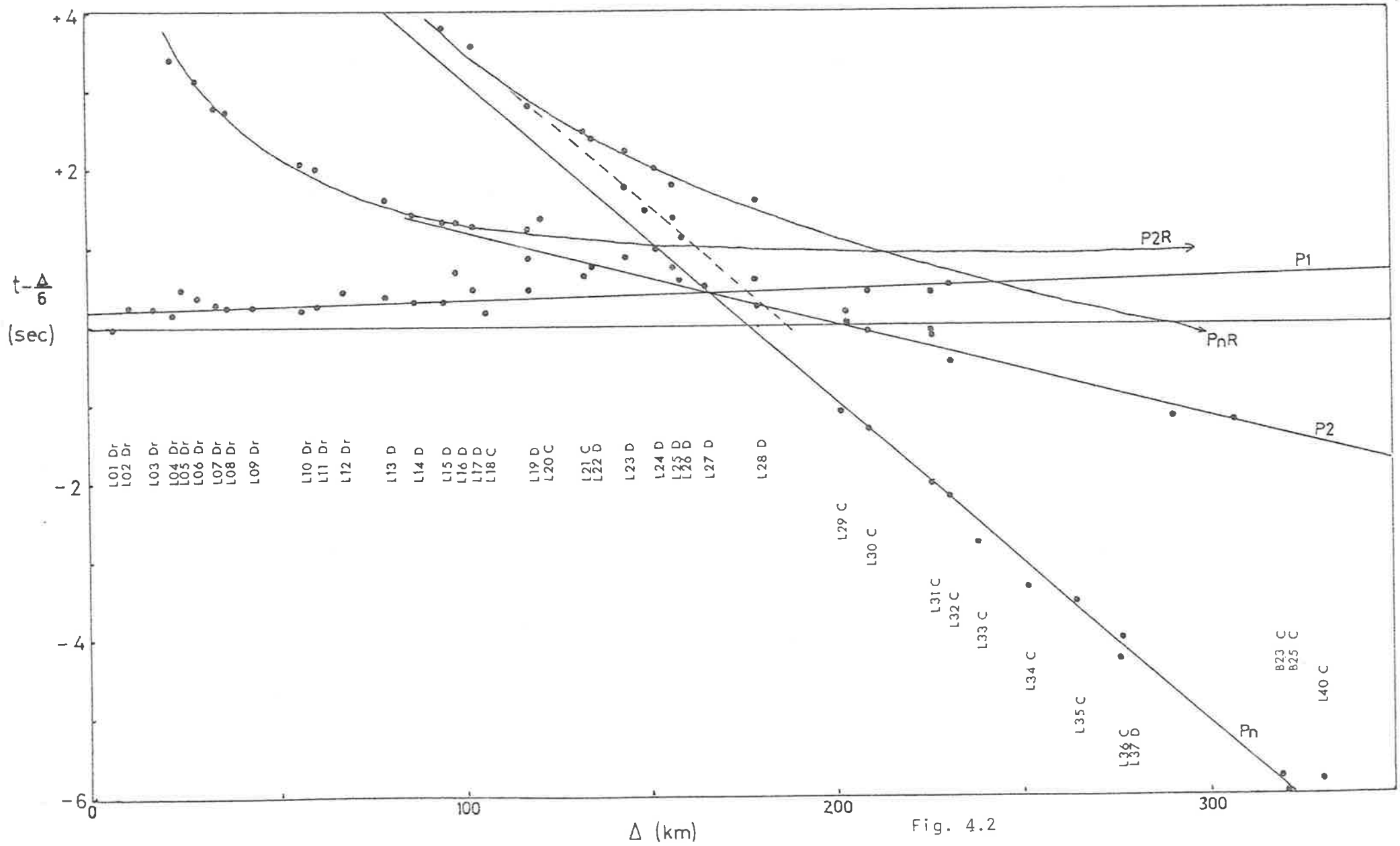
+4
+2
-2
-4
-6
0
100
200
300
t-Δ/6
(sec)
Δ (km)
P2R
P1
PnR
P2
Pn
L01 Dr
L02 Dr
L03 Dr
L04 Dr
L05 Dr
L06 Dr
L07 Dr
L08 Dr
L09 Dr
L10 Dr
L11 Dr
L12 Dr
L13 D
L14 D
L15 D
L16 D
L17 D
L18 C
L19 D
L20 C
L21 C
L22 D
L23 D
L24 D
L25 D
L26 D
L27 D
L28 D
L29 C
L30 C
L31 C
L32 C
L33 C
L34 C
L35 C
L36 C
L37 D
B23 C
B25 C
L40 C

Fig. 4.2

Figure 4.2 shows that the first arrivals define two travel time branches which intersect at approximately 170 km. The first arrivals before crossover are designated P1, while those beyond crossover are Pn. Three other sets of later P-wave arrivals have been identified on the LCK records. The first of these (P2R) appears with large amplitude between 70 and 160 km from the source, and can be traced back to 25 km, but with smaller amplitude. The second (PnR) is identified beyond 100 km. The amplitude characteristics of both P2R and PnR arrivals, the curvature of their travel time curves, and their high apparent velocities suggest that they are reflected phases arising from an intermediate crustal reflector and the Moho, respectively. The third set (P2) of later arrivals defines a linear travel time branch which appears to be tangential to the P2R curve. The P2 arrivals, which have been identified between 118 and 230 km, are never first arrivals on records of the LCK profile.

In accordance with the approach to interpretation stated above, linear travel time equations were fitted to the P1, P2 and Pn data, and hyperbolic equations to the P2R and PnR data. The travel time equations from which the squares of the deviations of the data are minimized are given in Table 4.1.

The travel times which were used to determine equation (1) were those of all first arrivals to 130 km, with the exception of the first arrivals at stations L16 and

L20 where, because of the need to use excessive attenuation due to high background noise level, the true first arrival was lost. Four later arrivals which were observed at stations L28, L30, L31 and L32, beyond the crossover distance for P1 and Pn, appear to be associated with the phase P1, and were included in the derivation of equation (1).

Table 4.1 Travel Time Equations for P wave data - LCK Profile

PHASE	TRAVEL TIME EQUATION	RMS RESIDUAL (SEC)	NO OF DATA	
P1	$t = \frac{x}{(5.95 \pm 0.01)} + 0.21 \pm 0.06$	0.08	22	(1)
P2	$t = \frac{x}{(6.42 \pm 0.04)} + 2.27 \pm 0.18$	0.12	13	(2)
Pn	$t = \frac{x}{(7.97 \pm 0.04)} + 7.33 \pm 0.16$	0.09	11	(3)
P2R	$t = \left(\frac{x^2}{(5.94 \pm 0.01)^2} + 39.88 \pm 0.88\right)^{\frac{1}{2}}$	0.09	12	(4)
PnR	$t = \left(\frac{x^2}{(6.21 \pm 0.03)^2} + 149.38 \pm 5.0\right)^{\frac{1}{2}}$	0.09	9	(5)

Other omitted first arrivals which occur before crossover, are those at stations L21 to L25, in the distance range 134 to 158 km from the source. These five arrivals all have large positive residuals from the travel time curve defined by arrivals at both nearer and more distant stations from the source. The continuity of the P1 branch to distances beyond the crossover distance suggests that the delays are better explained by near surface, rather than deeper structural effects, but this is not supported by an examination

of the surface geology in the vicinity of the anomalous stations, which indicates that essentially the same rock types exist along the whole profile. Nor is the explanation of the delays in terms of shallow structural effects supported by the good agreement between later (PnR) phases observed at the stations in question, and those observed at adjacent stations with "normal" P1 travel times. An alternative explanation of the large delays is that the anomalous first arrivals are not in fact P1. The loss of P1 in the distance range 134 to 158 km is consistent with the observed pattern of P1 amplitudes at smaller distances. At distances less than 70 km from the drain source, P1 amplitudes are large and onsets are sharp. Beyond 70 km, where the P1 records are predominantly of blasts at lobe D, the amplitudes of P1 are much smaller than for blasts at the drain site, although the charge sizes in both cases are comparable. The reappearance of P1 at distances beyond 200 km may be due to the fact that these records were of blasts in lobe C rather than lobe D. It has also been observed that no S1 phases were identified on records obtained from blasts at lobe D, although Sn was observed. It seems, therefore, that the loss of P1 (and S1) at stations L21 to L25 is due to the particular source being observed, rather than to either deep or shallow structural effects near the anomalous stations.

It should be emphasized that the above conclusion depends heavily on the association of the late arrivals at stations L28 to L32, with the P1 arrivals observed at

smaller distances from the source. If the distant arrivals are not in fact P1 arrivals, then the loss of P1 at stations L21 to L25 and beyond may be due to deep structural effects. In particular, the loss of P1 may be due to a velocity decrease with depth, as observed by Hales and Nation (1973) on their Rocky Mountain Profile, where P1 was not observed beyond 165 km. Branson et al (1972) have obtained evidence of a low velocity layer in the upper crust from a reflection survey in New South Wales, but apart from the loss of P1 arrivals mentioned above, there is no other evidence from the present study to support the existence of this low velocity layer in the geosyncline region. Several crustal models incorporating a low velocity layer have been studied in an attempt to account for the loss of P1 on the LCK profile. Constraints have been imposed on the models by the travel times of the phases P1, P2, P2R, Pn and PnR. As a result of these studies it has been found that a crustal model without an LVL best explains the travel time data, without however, accounting for the loss of P1. Additional evidence against the existence of an LVL has been found in the form of late phases which occur several seconds after the first arrivals at UMB and CLV from blasts at IB and Mt Fitton respectively. These late arrivals were registered at distances of 358 and 500 km from the respective sources and occur at the expected times for P1 arrivals. As a result of the above considerations it has been decided to include the distant late arrivals in the P1 data set, and to exclude an LVL from possible crustal models.

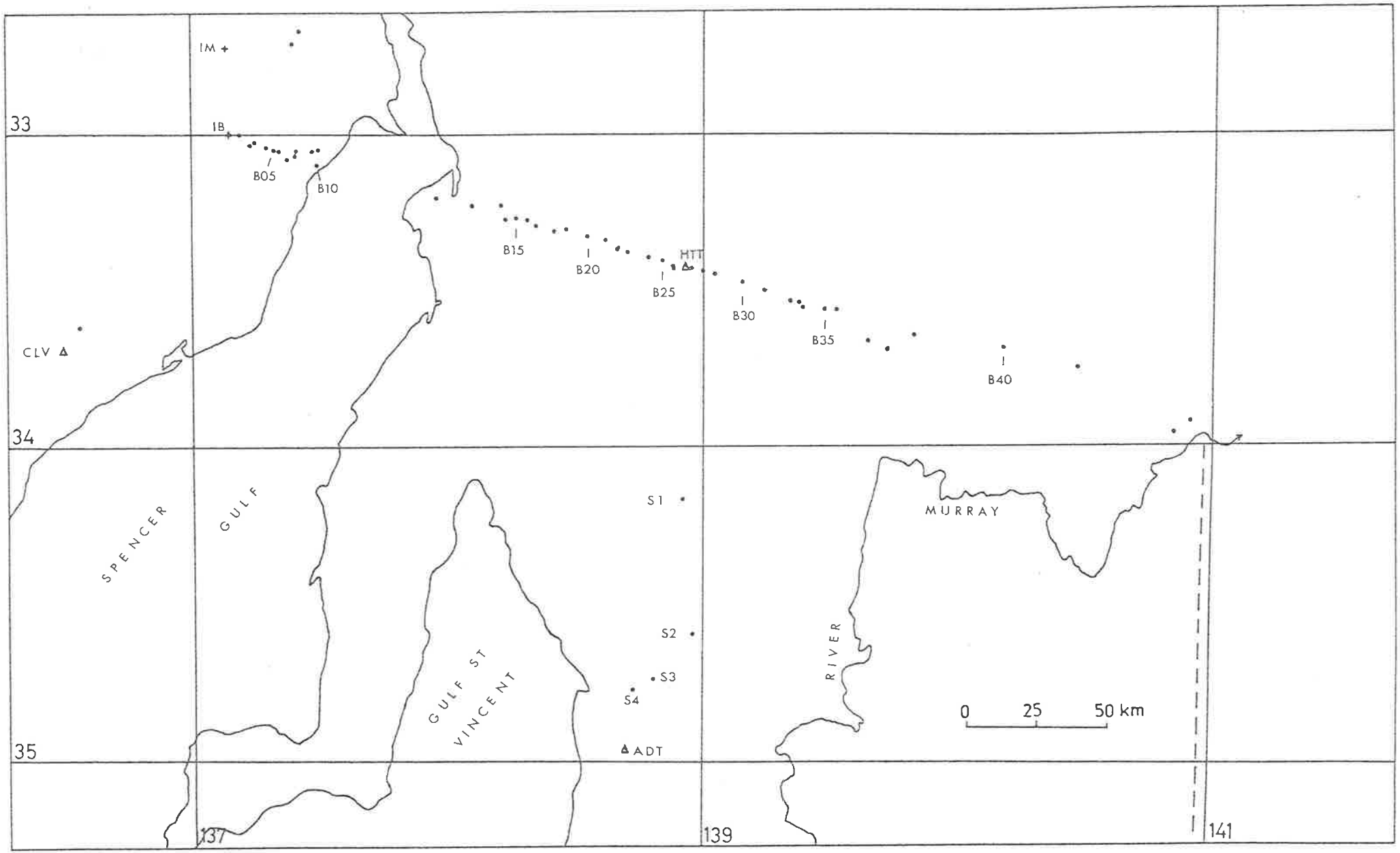

Figure 4.3 Distribution of stations recording arrivals from blasts at IB.

4.2.2 Iron Baron Profile

Fifty eight records were obtained along a profile (IB-E) 365 km long. The positions of the stations are shown in Figure 4.3. The travel times of P phases identified on these records are presented as a reduced travel time plot with a reducing velocity of 6 km/sec, in Figure 4.4. It can be seen from this figure that the first arrivals define three linear travel time branches, (P1, P2 and Pn), with crossover points near 100 km (P1, P2) and 210 km (P2, Pn) respectively. A set of large amplitude, later arrivals is also evident in the distance range 107 to 195 km. These arrivals appear to form an extension of the Pn curve. A selection of records from the IB-E profile which demonstrates these large amplitude second arrivals is shown in Figure 4.5. The break that exists in the record coverage between 33 and 78 km (stations B10 to B11) corresponds to the section of the profile occupied by Spencer Gulf. Two attempts to obtain records at sites in the gulf, using ocean bottom seismometers supplied by Flinders University were not successful. Linear travel time equations which were determined for the phases P1, P2 and Pn are given in Table 4.2. The data used to determine equation (6) were the travel times of the first arrivals at stations B1 to B14. Of the first arrivals associated with the Pn curve, those at the three most distant stations B41, B42 and B43 were omitted from the determination of equation (8) because of their anomalously early first arrivals (see Figure 4.4). An explanation of these observations will be offered below. The travel times to stations B16 and B17 were also omitted

Figure 4.4 Reduced travel time graph for phases observed on the IB-E profile best fit curve have been superimposed (Equations 6, 7 and 9 of Table 4.2).

t - Δ/6 (sec)
+4
+2
-2
-4
-6
-8
0
100
200
300
Δ (km)
B01
B02
B03
B04
B05
B06
B07
B08
B09
B10
B11
B12
B13
B14
B15
B16
B17
B18
B19
B20
B21
B22
B23
B24
B25
B26
B27
B28
B29
B30
B31
B32
B33
B34
B35
B36
B37
B38
B39
B40
B41
B42
B43
Pn
P2
P1

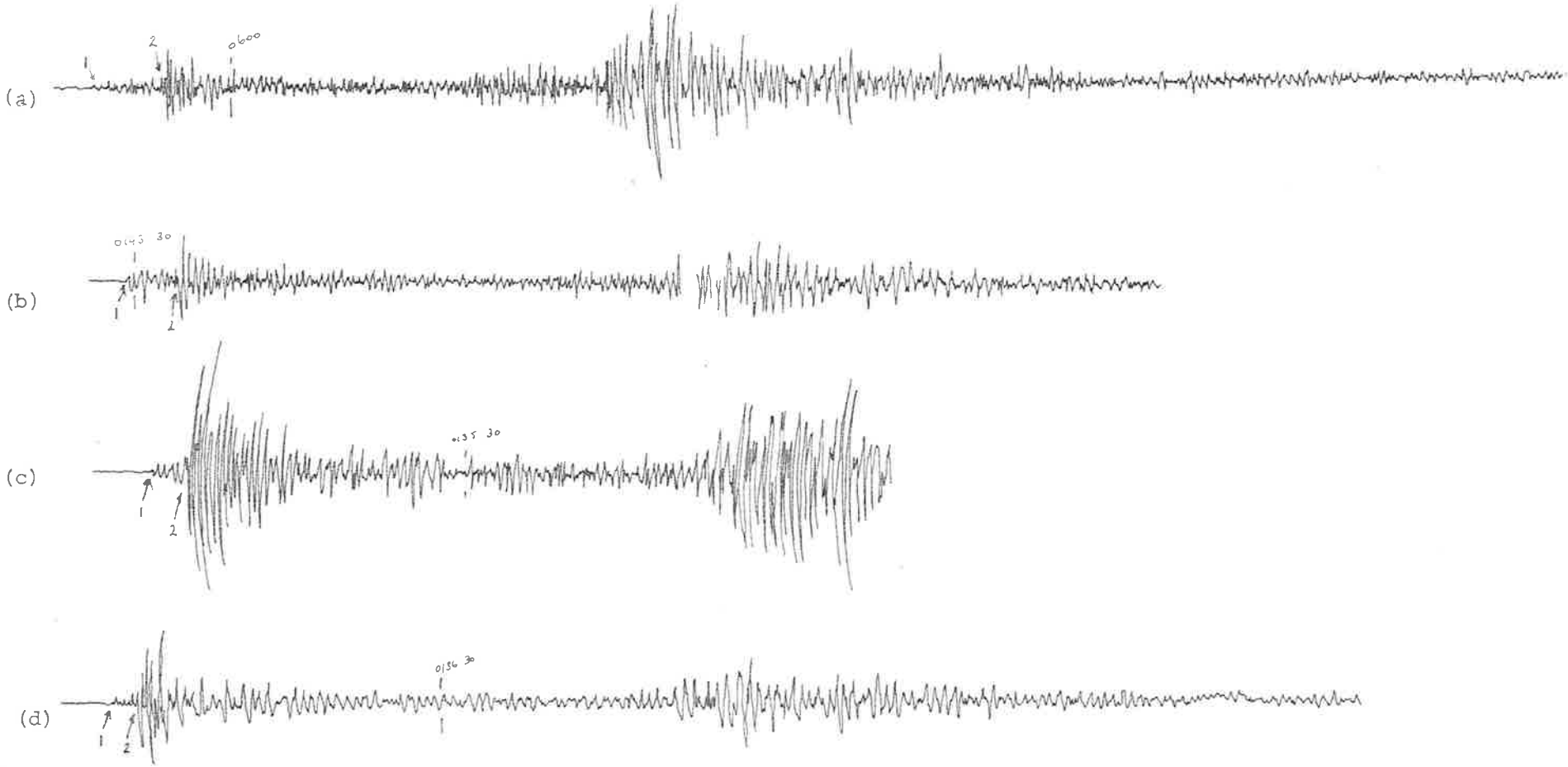

Figure 4.5 A selection of records which demonstrates the large amplitude second arrivals observed between 107 and 195 km on the IB-E profile. The records shown are from stations (a) B18 (b) B21 (c) B26 (d) HTT

from the determination of equation (7) because of their large (unexplained) positive residuals. When the travel times of the second arrivals observed between 107 and 195 km are taken together with the times of the Pn first arrivals, equation (9) of Table 4.2 is obtained.

Table 4.2 Travel Time Equations for P Wave Data - IB-E Profile

PHASE	TRAVEL TIME EQUATION	RMS RESIDUAL (SEC)	NO. OF DATA	
P1	$t = \frac{x}{(5.93 \pm 0.03)} + 0.23 \pm 0.04$	0.09	14	(6)
P2	$t = \frac{x}{(6.46 \pm 0.04)} + 1.59 \pm 0.13$	0.09	18	(7)
Pn (first arrivals only)	$t = \frac{x}{(8.03 \pm 0.13)} + 8.10 \pm 0.46$	0.16	11	(8)
Pn (first and later arrivals)	$t = \frac{x}{(7.97 \pm 0.03)} + 7.77 \pm 0.10$	0.10	27	(9)

4.2.3 Kanmantoo Profile

A small number of blasts were recorded at essentially two azimuths from the Kanmantoo Copper Mine. The westerly profile (KMT-W) which extented to 44 km from the mine toward the permanent station ADT, and incorporated 12 recording sites, provided good station coverage for the determination of shallow velocity structure. Records were also obtained at four stations lying north of KMT to a

Figure 4.6 Travel time graph for first arrivals from KMT blasts, observed at stations within 50 km of the mine. Solid line is best fit line for stations of the westerly profile (KMT-W) - Equation 10. Broken line is best fit line for northerly stations (KMT-N) - Equation 11.

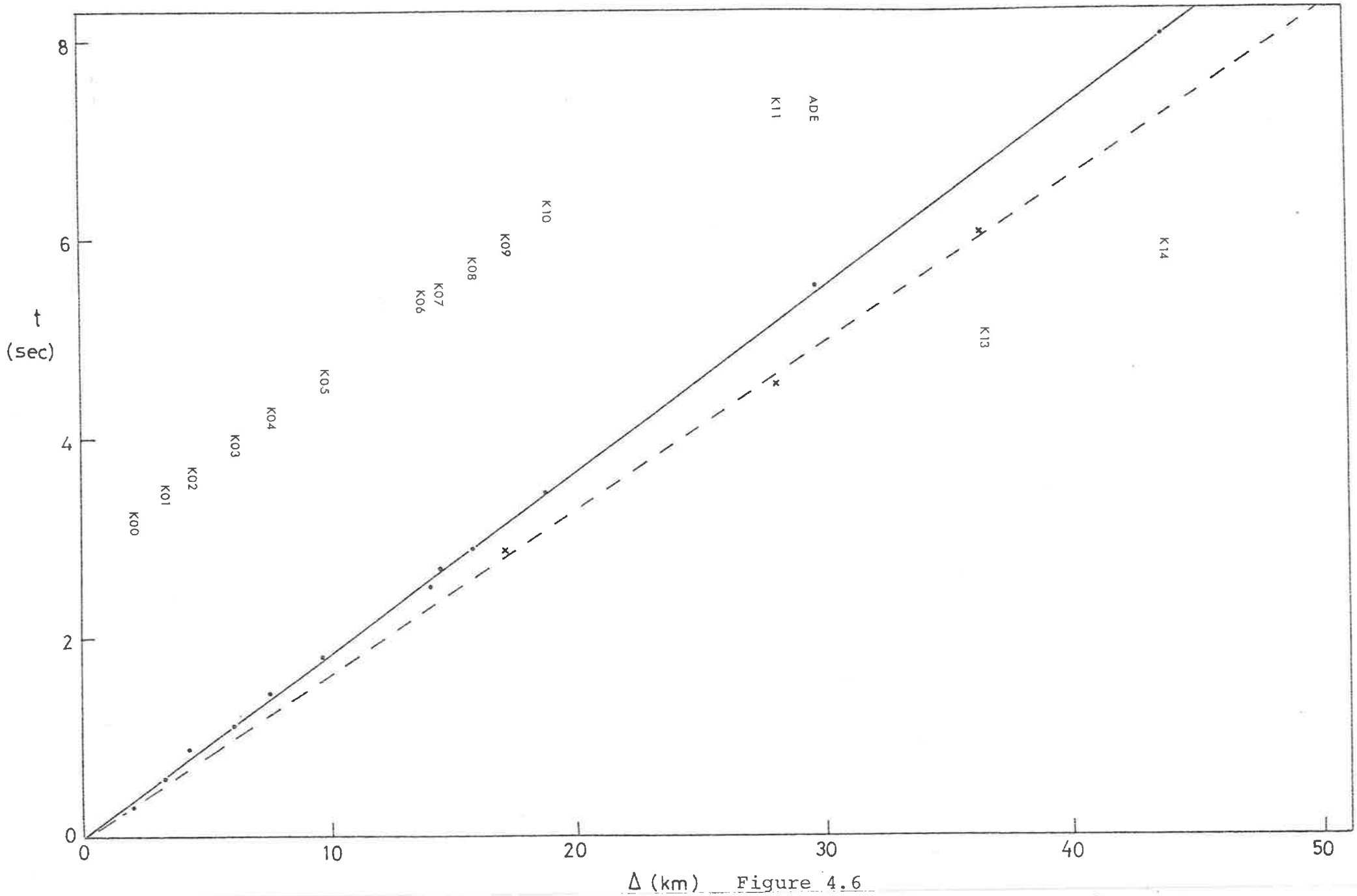
t
(sec)
0
2
4
6
8
0
10
20
30
40
50
Δ (km)
K00
K01
K02
K03
K04
K05
K06
K07
K08
K09
K10
K11
ADE
K13
K14

Figure 4.6

distance of 102 km from the mine. Travel times of first arrivals have been plotted for distances to 44 km in Figure 4.6, from which it is clear that even at small distances from the source markedly different velocities are required to describe the first arrivals for the westerly and northerly profiles, which define the solid and dashed lines respectively in Figure 4.6. The higher apparent velocity of the arrivals at the three northerly stations is consistent with the arrival at a fourth northerly station S1 (Δ=102 km) which is beyond the maximum distance shown on Figure 4.6. The residual of the travel time to this station, from equation (11), is 0.015 sec. The travel time equations for the two sets of P wave arrivals are equations (10) and (11) in Table 4.3.

Additional recording sites to the north of KMT were HTT, B41, B29, B27, B21 and B20 (see Figure 4.3), L31 and L30 (see Figure 4.1), which extended the northerly recordings to a distance of 308 km from the source. The recordings obtained at the seven most distant sites north of KMT were all obtained incidentally during attempts to record other blasts from either IB or LCK and hence the sites do not constitute a proper linear profile. In fact the disposition of the stations more nearly represents a fan spread of receivers relative to KMT. A difficulty encountered with such a deployment of stations is that of knowing whether the first arrivals at all stations have arisen from the same refracting horizon. As is observed in Appendix A.2 this problem besets all seismic experiments where phases cannot

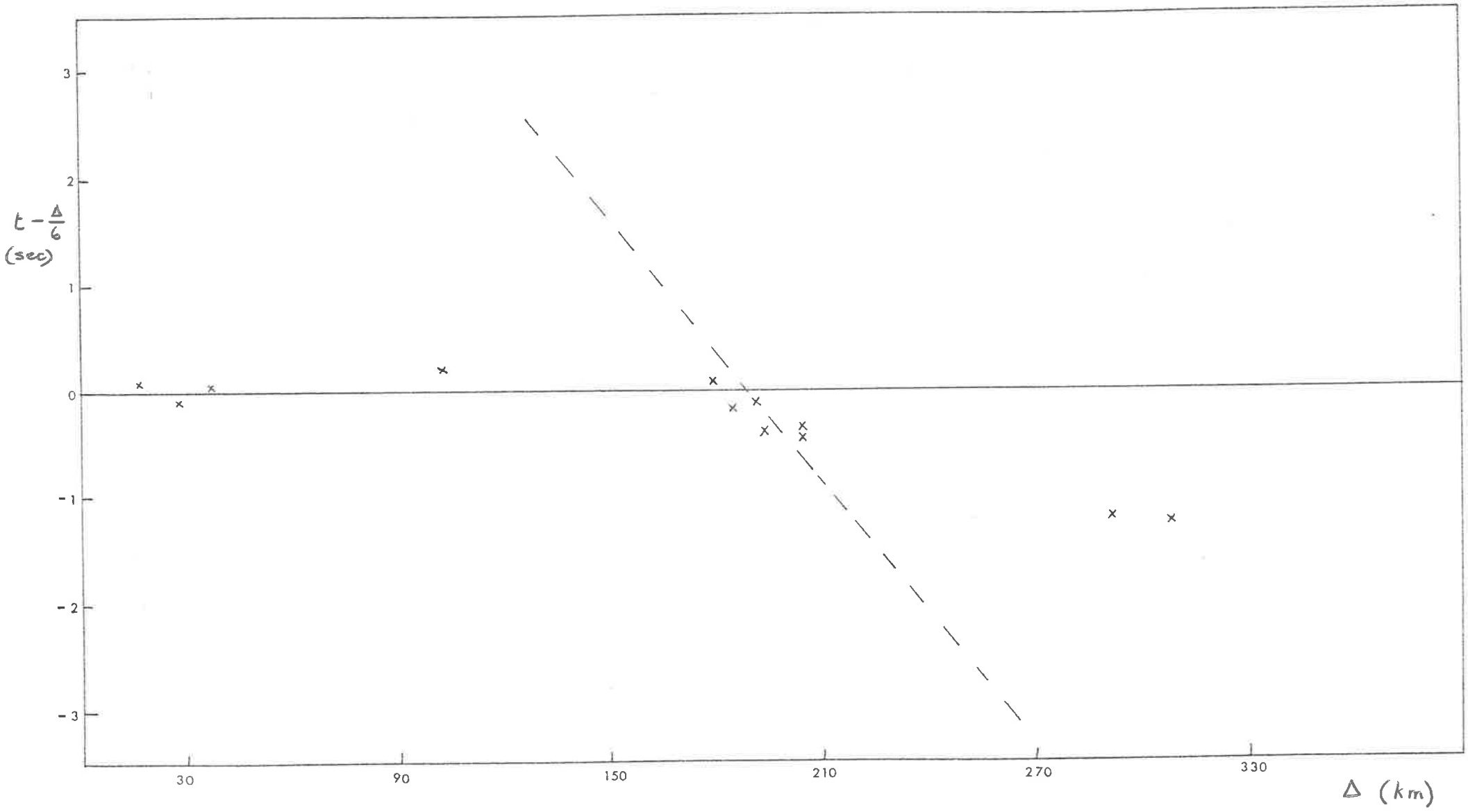

Figure 4.7 Reduced travel time plot for P data observed at stations north of KMT. Dashed line represents Pn travel times for IB profile.

be clearly traced from receiver to receiver. If, however, it is assumed that the arrivals do derive from a common refractor, then the apparent velocity of P waves in the refractor is 6.69 km/sec, as determined from the arrivals at stations HTT to B20 and excluding the two most distant stations. Clearly the distribution of stations between 178 and 204 km does not provide optimum conditions for an accurate evaluation of the refractor velocity. When the arrivals at the two most distant stations, which are of poorer quality than the nearer arrivals, are included, an apparent velocity of 6.36 km/sec is obtained. In this case the most distant arrivals tend to bias the data inordinately, so that in both attempts to group the KMT distant data the values for the refractor velocity must be treated with caution. It does appear, nevertheless, that although an accurate velocity has not been obtained, the value lies between the velocities determined for Pl and Pn arrivals on other profiles. The implication is that the arrivals at stations distant from KMT have arisen from an intermediate refractor. It should also be noted that Pn arrivals were not recorded at the two most distant recording sites L30 and L31. No explanation of this observation has been given. All northerly recordings of KMT blasts are plotted in Fig. 4.7.

Table 4.3 Travel Time Equations for P Wave Data - KMT Profiles

PHASE	TRAVEL TIME EQUATION	RMS RESIDUAL (SEC)	NO OF DATA	
Pl-westerly	$t = \frac{x}{(5.34 \pm 0.04)} + 0.00 \pm 0.02$	0.05	12	(10)
Pl-northerly	$t = \frac{x}{(5.92 \pm 0.06)} + 0.00 \pm 0.09$	0.07	4	(11)

4.3 Interpretation and Discussion - P-Wave Data

4.3.1 (a) Upper Crust - Shallow Sediments

The non-zero intercept terms of the P1 equations (1) and (6), suggest that a layer of low velocity material exists at or near the surface. Along both the LCK and IB profiles, the near surface material consists of sediments of Adelaidean age which are either apparent as outcrops or are covered by a thin layer of alluvium, so that the intercept terms of the P1 travel time equations may be attributed to the passage of seismic waves through shallow Adelaidean sediments. The sedimentary rocks which outcrop along both IB and LCK profiles are generally of Marinoan age (late Proterozoic) and consist of, in the main, shales, slates and sandstones. Press (in Handbook of Physical Constants (Pp 202 - 203)) has tabulated the results of seismic velocity measurements in sedimentary and metamorphic rocks, from several field and laboratory experiments. His table 9.4 gives sandstone - shale velocities of between 2 and 4.5 km/sec depending on age and depth of burial of the rocks (Press after Faust). The Adelaidean sediments of the Adelaide geosyncline are older than those considered by Faust, and therefore, by extrapolating from his observations, may be expected to have velocities higher than 4 km/sec.

In fact, from several seismic surveys which have been conducted by the South Australian Mines Department (B. Milton, personal communication), it appears that the mean velocity of P waves in Adelaidean sediments is significantly higher than 4 km/sec. These surveys, which were conducted

Table 4.4 P-Wave Velocities for Adelaide System Rocks (Compiled by B. Milton, South Australian Mines Dept)

AREA OF SURVEY	ROCK-TYPE	P WAVE VELOCITY (km/sec)
Blinman (Kendall)	Marinoan	
	Wonoka Fmn - shale, limestone	5.18
	Nuccaleena Fmn - dolomite	4.97
	Trezona Fmn - shale, limestone	5.03
Willochra Surveys	Marinoan	
	Willochra Fmn - siltstone	4.00
	Sturtian	
	Appila tillite, interbeds siltstone and sandstone	3.59
South of Lake Torrens (Kendall)	Marinoan	
	Tent Hill Fmn - siltstone, quartzite	4.88
Eucla Basin (Kendall)	Marinoan	4.42 - 5.03
Eastern Eucla Basin (Milton)	Adelaide System - undifferentiated	5.13
Port Augusta (McInerney & Roberts)	Adelaide System - undifferentiated	4 - 5
Redcliffs (Morony)	Adelaide System	4.87

in widely different regions of South Australia, yielded the velocities for Adelaidean sediments given in Table 4.4. The mean of the P wave velocities is 4.8 km/sec.

4.3.1 (b) Upper Crust - Crystalline Basement

The equations describing the P1 first arrivals on the LCK and IB profiles agree very well, both in their apparent velocity and intercept terms. These equations ((1) and (6)) describe the travel times of waves which have been refracted through the upper crust, and the intercept terms are due to the passage of waves through the shallow sediments described in the previous section. Velocities similar to those found in the present study for the phase P1, have been measured in four earlier studies in South Australia, and ascribed to material of the crystalline basement, an easterly extension of the Precambrian shield, which formed the floor of the Adelaide geosyncline. The earlier studies were made by Milton (1974, 1975), Kendall (196) and Doyle and Everingham (1964). A comparison of the earlier results with those of the present study provides a key to the interpretation of the phase P1.

Milton (1975) determined refraction velocities of 5.70 and 5.83 km/sec on two seismic refraction profiles east and west of the Karari Fault in the southwest Arkaringa Basin, where he found good agreement between depths to seismic, magnetic and crystalline basements, and was therefore led to associate the above velocities with crystalline basement.

Earlier work by Kendall (1967), who determined basement P velocities of between 5.6 and 6.0 km/s along several profiles, also in the Eucla Basin, defines the probable range of P velocities in the crystalline basement. It should be noted that Kendall's refractors agreed in depth with crystalline basement, as determined from borehole samples.

Finally, Doyle and Everingham (1964) found a shallow refractor with P-wave velocity in the range 5.70 to 5.88 km/sec at three of the recording sites, and at the blast site of the 1956-7 Maralinga atomic tests. This refractor was identified at each of the four sites by local seismic surveys which were made for the express purpose of determining shallow structure and hence station corrections, for the broader scale work. At the Maralinga blast site the depth to the refracting horizon was found to be 440 m, and drilling intersected Archaean basement at a depth of 525 m (Ludbrook (1961)), so that the refractor was identified as crystalline basement. In their broader scale work, however, Doyle and Everingham found a Pl velocity of 6.3 km/sec from seven first arrivals recorded over a distance of 187 km. The different velocities found in the small and large scale surveys were reconciled by assuming an increase of velocity with depth in the crystalline material. Such an increase of velocity is expected to occur in the shallow crust as porosity of the near surface rocks decreases, and pressure increases (Steinhart and Meyer (1961)). Because of the very small intercept of the 6.3 km/sec branch and its continuity to large distances, they

concluded that the velocity must increase very rapidly at shallow depths, and subsequently remain essentially constant over the remainder of the crust. By contrast, in the present study P1 arrivals were recorded as first arrivals to a distance of 130 km on the LCK profile and 104 km on the IB profile, and beyond crossover P1 could be identified to 231 km on the LCK profile, without any evidence of a strong velocity gradient producing P velocities in excess of 6 km/s, as suggested by Doyle and Everingham.

In the light of the four earlier studies which ascribed a velocity of 6 km/s to crystalline basement material, it would perhaps seem appropriate to also associate the phase P1 of the present study with crystalline basement. Given the P-wave velocity of 5 km/sec in the sediments overlying basement in the Adelaide geosyncline, the intercept terms of the P1 travel time equations (equations (1) and (6)) then yield depths to the basement refractor of the order of one kilometer. However, such a shallow depth to basement along the LCK profile does not agree with the depths to magnetic basement determined by the Bureau of Mineral Resources and published in the form of a 1:1 000 000 Contour Map of Depth to Magnetic Basement. According to this source, magnetic basement increases in depth from 1 to 6 km in the first 50 km of the LCK profile, and exists at depths in excess of 7 km for the remainder of the profile. There is no evidence from the P1 apparent velocity to suggest that the P1 arrivals have arisen from a down-dipping refractor. On the Eyre Peninsular section of the IB profile, on the other

hand, magnetic basement occurs at a depth of less than 1 km and yet the P1 travel time equation has essentially the same value of intercept term as for the LCK profile. It is clear that if the interpretations of crustal structure from magnetic, seismic and geological observations are to be consistent, then either magnetic and crystalline basements are coincident, in which case the seismic horizon is not crystalline basement, or the magnetic and crystalline basements are not coincident. Because of the good correlation between magnetic and crystalline basements where depths to the latter have been determined from drilling or outcrops, and because of the thickness of sediments known to exist in the Adelaide geosyncline, it would seem most likely that crystalline and magnetic basements do both exist at depth in the central geosyncline region and hence that the seismic horizon associated with equations (1) and (6) is not Precambrian crystalline basement, as may have been supposed from velocity considerations alone.

In addition, Stewart has estimated that the thickness of the Adelaidean sediments ranges up to 6 km in the southern part of the Adelaide geosyncline, in agreement with depths to magnetic basement, and that the P wave velocity in the sedimentary material is approximately 4.5 km/s. If the velocity of the basement material which underlies the sediments is taken to be 5.95 km/s, as is indicated by the P1 arrivals on the LCK and IB profiles, then the crossover distance for the sedimentary and basement arrivals would be 33 km, assuming horizontal, uniform layering, and a thickness of 6 km for the sediments. None of the recorded first arrivals on any profile, however, exhibit the low apparent

velocity indicative of direct ray paths through the low velocity sediments. In fact, first arrivals at ten stations within 20 km of the KMT source have an apparent velocity of 5.42 km/s. The travel time equation which has been fitted to the data from KMT has zero intercept and the data have an RMS residual of 0.05 sec from the line of best fit. Although it may be argued that the high velocity is due to the high degree of metamorphism of the rocks in the Kanmantoo Trough, compared to the shallow sediments in the northern part of the Adelaidean geosyncline, it is also true that the few arrivals observed at stations within 20 km of the LCK and IB blasts fit the KMT travel time curve. Since the waves producing these arrivals will have traversed a relatively shallow layer of sedimentary material, then the P wave velocity in the sediments, even at depths of less than 1 km, must be significantly higher than 5 km/s. This would suggest that in the Adelaide geosyncline generally, the P wave velocity increases rapidly with depth near the surface.

Furthermore, failure to observe phases which had been reflected from the top of the basement may be taken as evidence against the existence of a sharp velocity discontinuity at the bottom of the sedimentary column, which a uniform layered model would predict. It is therefore suggested that the P1 equations (1) and (6) describe waves that have been continuously refracted in a crust where the P wave velocity increases rapidly from 5 km/sec in the near surface Adelaidean sediments, to about 5.8 - 5.9 km/sec at

a depth of one or two kilometres, and continues to increase more gradually at greater depths in the deeper sediments and crystalline basement.

4.3.2 An Intermediate Velocity Discontinuity

Evidence for the existence of a first order discontinuity of seismic velocity at intermediate depths in the crust, is provided in this survey by four sets of arrivals. The first is the phase P2R which was observed on the LCK profile. The P2R arrivals, which are shown in Figure 4.2, are described by equation (4). The phase has been identified as a reflected phase by virtue of its amplitude characteristics, the curvature of its travel time branch and the high apparent velocity of the arrivals at small distances from the source. The value of 5.94 km/sec which occurs in the denominator of equation (4) represents an average velocity of P waves in the section of the crust traversed by the P2R waves. This average velocity is in very good agreement with the refraction velocity determined for the phase P1 (equations (1) and (6)), and supports the earlier suggestion that the upper crust is essentially uniform, except for a strong velocity gradient in the near surface zone. The constant term of equation (4) yields a depth to the reflector of 18.8 km, subject to the assumption of a uniform upper crust. The failure to observe corresponding P2R arrivals on the IB profile was due, in part, to the missing section of that profile corresponding to Spencer Gulf.

The second set of arrivals observed on the LCK profile, which may be considered as evidence for an intermediate reflector/refractor, is the phase P2, which is also shown in Figure 4.2, and described by equation (2). The P2 travel time branch is tangential to the P2R curve and linear, suggesting that the phase P2 consists of arrivals of waves which have been critically refracted at the top of a lower crustal layer, whose P velocity is 6.42 km/sec. By assuming the upper crustal parameters deduced in previous sections, the depth to the (horizontal) refractor is found to be approximately 18 km, which agrees with the depth to the reflector giving rise to the P2R phase.

The third set of arrivals which affords perhaps the most convincing evidence for a velocity discontinuity in the crust, is the set of first arrivals observed on the IB profile between stations B13 and B33 over a distance range of approximately 110 km. These arrivals which are shown in Figure 4.4, are described by equation (7). The good agreement between the apparent velocity of this phase (6.46 km/sec) and the P2 arrivals observed on the LCK profile implies that both sets of arrivals have arisen from the same high velocity refractor, in which the P velocity is 6.46 km/sec, and that the refractor is horizontal, at least over those parts from which the observed P2 arrivals are refracted back to the surface. However the travel time equation for the phase P2 which is observed along the IB profile, has a smaller intercept term than the corresponding P2 equation for the LCK profile (equations (7) and (2) respectively).

The depth to the horizontal refractor along the IB profile, assuming uniform, horizontal layering, is 12 km, compared with 18 km for the LCK profile.

The fourth set of arrivals which may be associated with the intermediate refracting horizon is a set of first arrivals at eight stations lying between 182 and 308 km north of KMT. These arrivals were discussed in Section 4.2.3 above and the rationale for their association with the intermediate refractor was given there. Since certain of the stations which recorded KMT arrivals also recorded P2 arrivals from both IB and LCK it was possible to use a simple time term approach to obtain the contour of the refractor along parts of the IB-E and LCK-S profiles. This procedure required the assumptions that the arrivals at the stations north of KMT were P2 refracted arrivals and that azimuthal effects were negligible insofar as they affected station and source time terms. The model on which the analysis was based consisted of a uniform upper crust of P wave velocity 5.95 km/s overlying a refractor of P velocity 6.46 km/s. The model of the upper crust was that obtained from P1 and P2R arrivals; the velocity assumed for the lower crustal material was that determined from the P2 first arrivals on the IB-E profile, and the phases P2 and PnR on the LCK-S profile. The phase PnR is discussed below in Section 4.3.3. The method involved computation of station and source time terms which were then interpreted in terms of variations in the depth to the intermediate refractor.

The LCK source time term was initially calculated to be 1.23 sec, using the depth to the reflector obtained from the P2R travel time curve and the crustal model described above. It is interesting to note that this value is equal to one half of the average intercept term for the twelve stations which observed P2 refracted arrivals from LCK. This indicates that the refractor is essentially horizontal along the LCK-S profile. From knowledge of the LCK source term it was a simple procedure to evaluate station terms for stations observing P2 arrivals on the LCK-S profile, and subsequently the KMT source term from stations which observed P2 arrivals from both LCK and KMT. Likewise, station terms were evaluated for stations which observed both IB and KMT blasts and finally the IB source term was obtained. It should be pointed out that the stations involved were relatively few, and for this reason the results must be viewed with caution. Notwithstanding this caution, the time terms indicated that the intermediate refractor was not horizontal over its entirety. When the time terms were interpreted in terms of depths, using the assumed crustal model, the depth to the refractor was found to increase from approximately 14 to 19 km between stations B20 and L30 on the KMT profile. This increase of depth is consistent, of course, with the biassing effect of the arrivals at L30 and L31 in producing a lower apparent velocity for P2, as discussed in 4.2.3 above. Furthermore, the IB source term appeared to be smaller than the average of the station terms along the IB profile. The increased value of time term for the stations of the profile compared to the IB source term

corresponded to an increase of depth to the refractor of 4 to 5 km in the vicinity of Spencer Gulf. This increase in depth to the refractor may occur over a distance range of approximately 50 km between 20 and 70 km from IB, which are the offset distances for critically refracted waves from the source and station B13 respectively. Station B13 is the first station along the IB profile to record a P2 arrival.

The postulated increase in depth to the refractor along the IB-E profile is consistent with the increase in depth to magnetic basement which occurs at the eastern edge of Spencer Gulf. The depth to magnetic basement increases from 250 metres at the eastern edge of the gulf to 7.5 km in the mid-geosyncline region (see Figure 4.9). It is therefore suggested that the profile of magnetic basement, which probably corresponds to crystalline basement, is paralleled by the contour of the deeper refracting horizon, so that both horizons suffer either marked downwarping or downfaulting at the western edge of the geosyncline.

Additional evidence for the existence of a shallow reflector to the west of Spencer Gulf has been obtained from second arrivals at four stations within 33 km of IB. The high apparent velocity of these later arrivals suggest that they are reflections from a reflector at a depth of approximately 8 km, with a critical distance of 30 km. It is interesting to note that the most prominent arrival in this set of suspected reflections is the arrival at station B10

at a distance of 33 km from the source. It is also possible that high P1 velocity observed by Doyle and Everingham across Eyre Peninsula is, in fact due to the high speed refractor occurring at even shallower depths in the vicinity of Maralinga.

Independent evidence for an intermediate crustal reflector has been produced by Branson, Moss and Taylor (1972) who, in trial experiments to establish procedures for recording deep crustal reflections, recorded arrivals at near vertical incidence, with two way reflection times of 5.0, 11.3 and 14.6 secs, near Broken Hill, N.S.W. (Figure 2.1). Their interpretation of the events placed a reflecting discontinuity at a depth of 15 km, with an average P wave velocity above it of 5.9 km/sec, in close agreement with the observations of the present study. A second trial at Mildura, Victoria gave a similar result, with an intermediate reflector again being a prominent feature of the interpretation. Possible structure in the crust above the reflector at Broken Hill, including a low velocity layer, has not been confirmed in the present study.

4.3.3 Lower Crust and Upper Mantle

Beyond approximately 150 km on the LCK profile, and 200 km on the IB profile, the first arrivals define linear travel time segments, with apparent velocities which indicate that the waves have been critically refracted at the Moho. When prominent second arrivals, observed

on records of the IB profile between the critical and cross-over distances (approximately 100 and 200 km from the source respectively), are included in the Pn data set for that profile, then the Pn arrivals for both LCK and IB profiles have apparent velocities which agree very well (equations (3) and (9)).

In addition to Pn arrivals which were intentionally recorded along the IB and LCK profiles, several blasts from IB and IM were recorded inadvertently at sites along the LCK(N-S) profile. These records will subsequently be referred to as IB-N and IM-N records. Eight IB-N records were obtained at distances from IB such that the first arrivals were undoubtedly the phase Pn. The eight records were recorded at stations L07, L09, L12, L18, L20 L21 and UMB (see Figure 4.1). When the extra data are added to the IB-E Pn arrivals, no change is produced in the Pn travel time equation (9). Thus the ability of equation (9) to describe Pn arrivals over a broad range of azimuths from IB, and the agreement between the apparent velocities of Pn arrivals observed along both the LCK-S and IB-E profiles, suggests that the true velocity of P waves in the upper mantle is 7.97 km/s, which is in good agreement with the value determined by Stewart (1971) (Table 1.1). Furthermore, the good agreement between the apparent velocities for Pn along the two profiles suggests that the Moho is essentially horizontal in those areas from which the observed Pn arrivals are refracted back to the surface, that is, over the areas mapped by the offset positions from the stations

recording Pn arrivals from each source.

In addition to the eight IB-N first arrivals, several events were recorded at stations along the LCK profile from blasts from IB and IM, but within the crossover distance from the sources. These records feature prominent second arrivals similar to those observed on the IB-E profile (see Figure 4.5), at distances between the critical and crossover points on that profile. When these later arrivals are associated with the Pn branch, together with the corresponding arrivals on the IB-E profile, the mean intercept term, for a Pn velocity of 7.97 km/sec is found to be 7.75 ± 0.25 sec (N=67), where the error term is the standard deviation of the mean intercept value.

For the eleven Pn first arrivals on the LCK profile, the mean intercept is 7.31 ± 0.09 sec (N=11). However, a further five arrivals which occur before crossover on the LCK profile have a mean intercept of 7.75 ± 0.05 sec. It should be noted that the five arrivals, which fit the dashed line in Figure 4.2, were not included in the determination of equation (3) because of their large delays from the curve defined by the Pn first arrivals. The first arrival at the permanent station PNA, from LCK has an intercept term of 7.70 sec, and a LCK blast recorded at two sites near IB (see Figure 4.8) gave intercepts at those stations of 7.66 and 7.75 secs. In Figure 4.8 the intercept terms are plotted at station positions for each station along the LCK profile which recorded a Pn arrival from either IB or LCK, or both sources. The underscored figures

Figure 4.8 Map showing "intercept" values, $T-\Delta/7.97$, for Pn arrivals plotted at station positions. Underscored values indicate the intercepts of Pn arrivals from LCK blasts.

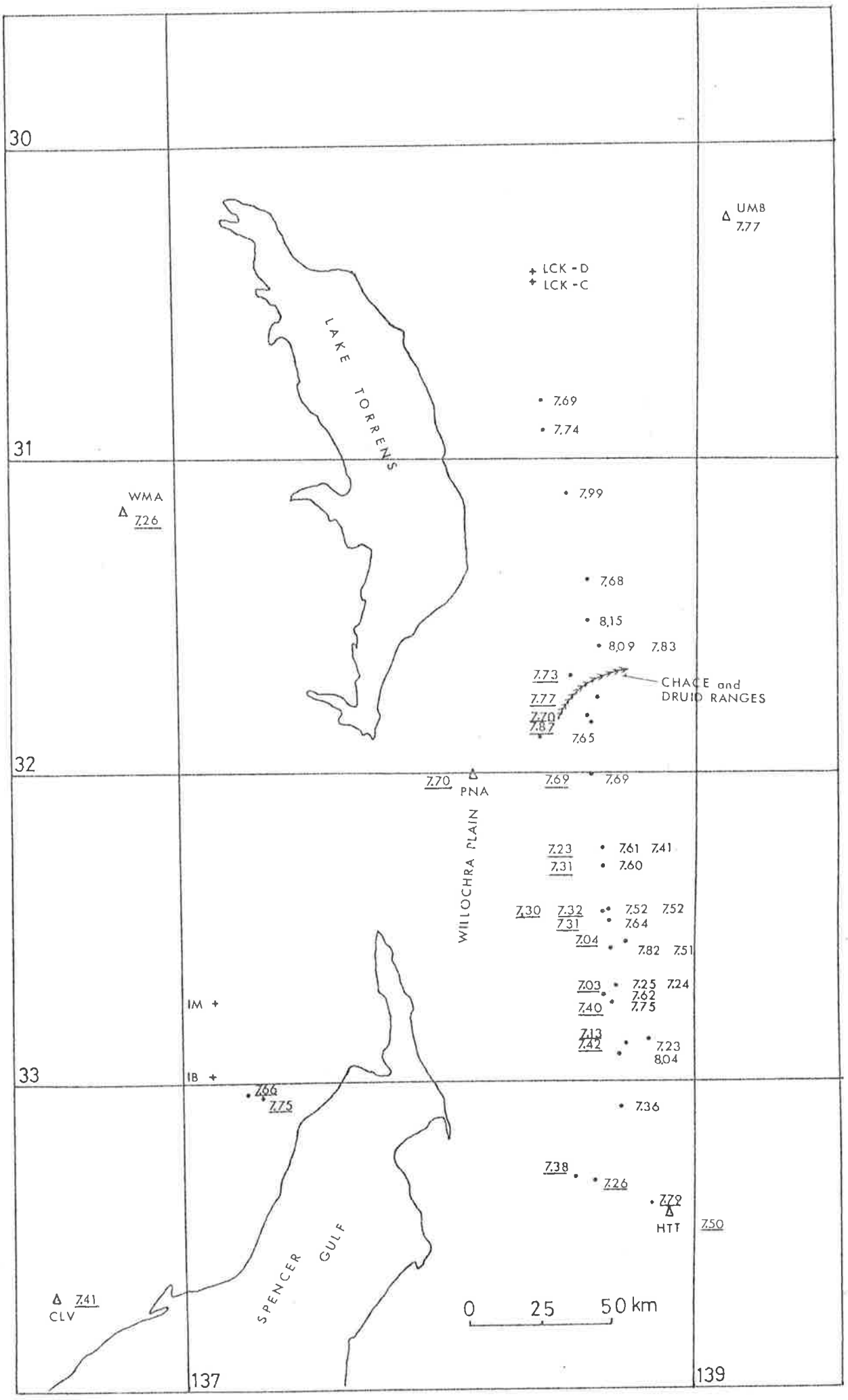
30
31
32
33
137
139
LAKE TORRENS
WILLOCHRA PLAIN
SPENCER GULF
UMB
7.77
LCK - D
LCK - C
7.69
7.74
WMA
7.26
7.99
7.68
8.15
8.09
7.83
7.73
7.77
7.70
7.87
7.65
CHACE and
DRUID RANGES
7.70
PNA
7.69
7.69
7.23
7.31
7.61
7.41
7.60
7.30
7.32
7.31
7.52
7.52
7.64
7.04
7.82
7.51
7.03
7.25
7.24
7.62
7.40
7.75
7.13
7.42
7.23
8.04
IM
IB
7.66
7.75
7.36
7.38
7.26
7.29
HTT
7.50
CLV
7.41
0 25 50 km

Figure 4.8

are the intercepts of Pn arrivals from LCK blasts.

From the pattern of intercept values evident in Figure 4.8, it appears that the Pn first arrivals recorded at stations more distant than PNA on the LCK profile, have arisen from a shallower refractor than Pn arrivals recorded either at closer stations on the same profile, or from blasts at IB and IM. Neglecting the six observations including that at PNA, for which intercept terms from LCK blasts averaged 7.75 sec, it is tempting to attribute the large intercepts observed for IB blasts to a large time term for the IB, IM sources, compared with the source time term for LCK. Inclusion of the six LCK observations (dashed line Figure 4.2), however, demands an alternative explanation. It would seem, rather, that a decrease in the depth to the Moho occurs between stations L28 and L29 on the LCK profile (see Figures 4.1 and 4.8). The postulated decrease in Moho depth would occur in the vicinity of the Chace and Druid Ranges, which lie at the northern edge of the Olary arc near Hawker, and separate two regions of folding. The fold axes to the north of the Chace and Druid Ranges are generally oriented north-south; those immediately south of the ranges have east-northeast trends, following the Olary arc.

Since Pn arrivals at stations lying south of the Chace and Druid ranges, from blasts at IB and IM, have intercept times typical of IB blasts recorded in other areas, then the western edge of the postulated uplift of the Moho must lie

nearer to these stations than the offset distance for Moho refracted arrivals. That is, the western edge of the uplifted Moho must lie within 50 km approximately, of the stations L29 to L40, in a westerly direction. It appears that the Willochra Plain may mark the western edge of the uplifted area. The southern extent of the uplifted Moho is unde termined, but it cannot extend as far south as the IB-E profile, which lies at approximately latitude $33^{o}15'$ South, since intercept terms for Pn along this profile are "normal" for IB blasts. The smaller intercept term for the LCK profile, beyond station L29 corresponds to an uplift of the Moho of approximately 4.5 km, with respect to an average overall depth of 38.5 km. These estimates of depths are based on assumptions of horizontal and uniform layering in the crust. It is of interest to note that Stewart (1972), in a statistical study of earthquake residuals over one degree areas of South Australia, found that the crust was thinner in the unit area from latitude 32^{o} to 33^{o} South and longitude 139^{o} to 140^{o} East, than the average crustal thickness in South Australia. This unit area borders on, and possibly includes part of the Moho which the present results also indicate is uplifted. Although the vertical extent of the uplift found in the present study is almost three times that found by Stewart, it is possible that the large area studied, and the nature of the data (earthquake data) used by Stewart resulted in an averaging and hence reduced value for the extent of uplift, while still preserving the trend.

The phase PnR, which has been interpreted as a reflection from the Moho, supports the suggestion that the Moho is deeper in the northern part of the LCK profile than it is further south. From Figure 4.2 it can be seen that when the Pn first arrival branch, is extrapolated back to 100 km, it is considerably earlier than the PnR curve, to which it should be a tangent, but the dashed line, which marks the five supposed Pn observations before crossover, is tangential to the reflection curve. The phase PnR also provides evidence that the P-velocity in the lower crustal layer is essentially constant, for just as evidence that the upper crust was uniform was drawn above from P1 and P2R apparent velocities, the phases P2 and PnR provide similar evidence with respect to the lower crust. From equation (5), the average velocity for the crust traversed by PnR waves is 6.21 km/s. If the velocity in the lower crust is assumed to be constant, then the velocity and thickness of the lower crustal layer which minimize the PnR residuals are 6.46 km/s and 19.6 km respectively. This value of the average velocity in the lower crust is in agreement with the velocity determined independently from the P2 arrivals on both LCK and IB profiles, and thus supports the assumption that the lower crust is uniform.

Finally, mention should be made of the three first arrivals recorded at stations B41, B42 and B43 on the IB-E profile. As can be seen from Figure 4.4, the three arrivals are early by approximately 0.5 sec, with respect to the Pn branch (equation (10)) defined by other Pn arrivals at

Figure 4.9 Depths to magnetic basement in the vicinity of the IB-E profile - 500 metre contours.

- ● Seismic stations B40 to B43
- o Offset positions from these stations

(Map adapted from map prepared by Bureau of Mineral Resources)

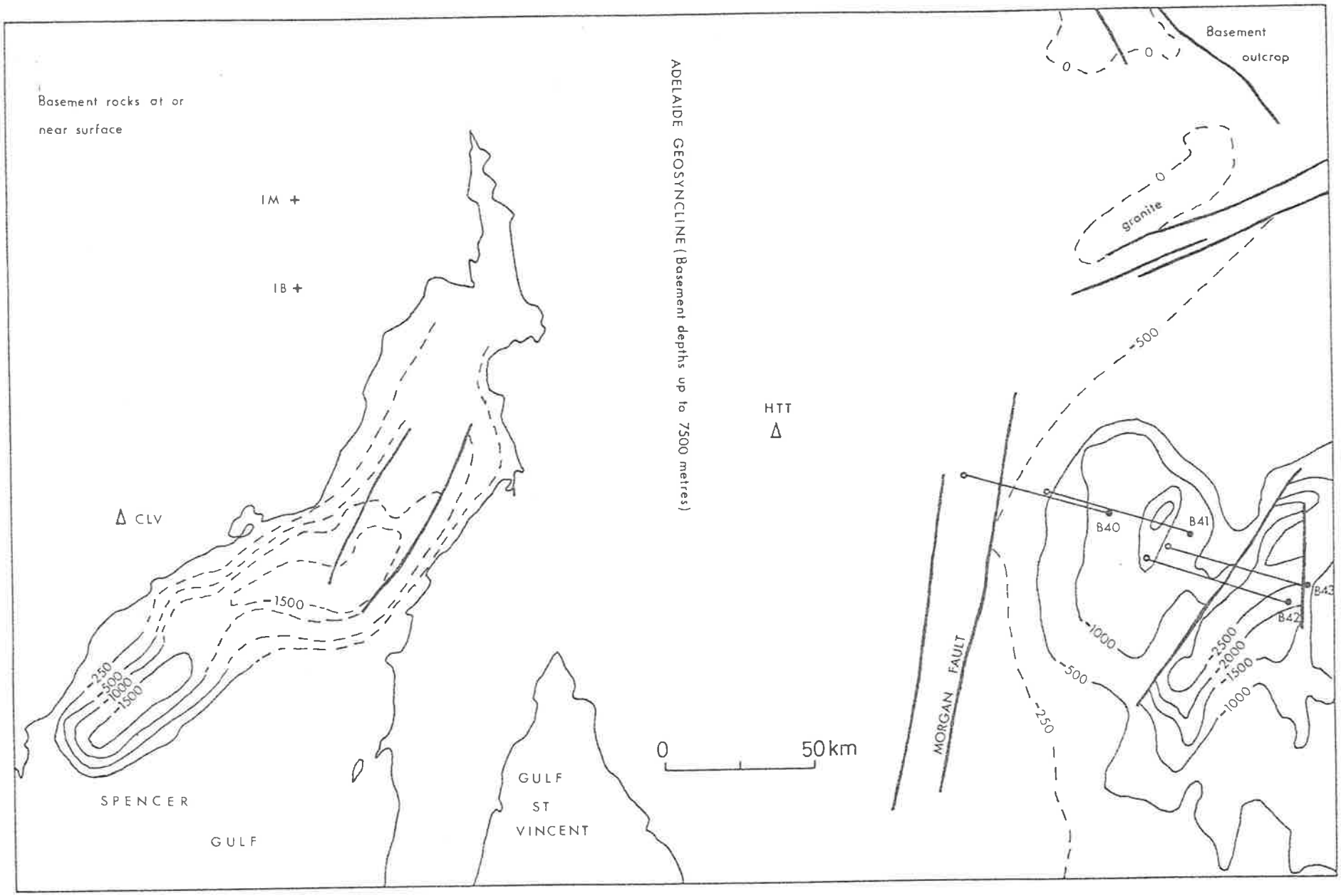
Basement rocks at or near surface
IM
IB
CLV
HTT
ADELAIDE GEOSYNCLINE (Basement depths up to 7500 metres)
Basement outcrop
granite
0
500
1500
250
500
1000
1500
2500
2000
1500
1000
500
250
B40
B41
B42
B43
MORGAN FAULT
SPENCER GULF
GULF ST VINCENT
0
50km

Figure 4.9

stations nearer to IB. An interpretation of the anomalous arrivals in terms of variation in depth to the Moho required a decrease in depth of the order of five kilometres in the vicinity of station B41. It can be seen from Figure 4.9 that the offset positions from stations B40 and B41, toward IB, lie to the west and east of the Morgan Fault respectively (see Figure 4.9). It can also be seen that the Morgan Fault marks the eastern edge of a region of very deep magnetic basement, so that to the west of the Morgan Fault, magnetic basement occurs at depths up to 7500 metres, while to the east, magnetic basement occurs at a depth of less than 1000 metres. It seems, therefore, that the decrease in depth to magnetic basement which occurs at the Morgan Fault may correspond to a decrease in depth to the Moho of several kilometres, and that as suggested above, the arrivals at stations B41 to B43 are early because of this decrease in depth. This explanation of the anomalous arrivals implies that the Morgan Fault is a major basement fault.

4.4 Travel Times of Shear Waves

Although shear waves often have large amplitudes on seismic records, their onsets are generally difficult to locate accurately because of the continuing ground motion following the earlier P wave arrivals, which obscure the S wave onset. In spite of this difficulty, shear wave arrivals have been identified on records of both the IB-E and LCK profiles.

4.4.1 Leigh Creek Profile

The first set of shear wave arrivals which was identi-

fied on the LCK profile had sharp onsets. Ten arrivals were read from records of drain blasts, out to a distance of 68 km. The linear equation which has been fitted to these travel times is given as equation (12) in Table 4.5. Now the variation with distance of residuals from equation (12) of the S wave travel times, correlates very well with that of P wave residuals from equation (1). A plot of the travel time differences between S and P phases ($t_s - t_p$) against P travel times (t_p) for the ten stations gave a ratio of P to S velocities of 1.72 ± 0.01. The RMS residual of the data from the linear relation was 0.04 sec. Furthermore, for each station at which both P1 and S1 arrivals were recorded, the S wave residual from equation (12) was invariably greater than the P wave residual from equation (1), and in the same sense, suggesting that both sets of residuals are due to a common cause. The possible causes of travel time residuals are

(1) errors in reading arrival times,

(2) errors in the origin times of the blasts,

(3) errors in the clocks at the recording stations,

(4) errors in the source to station distances, or

(5) velocity differences from the average velocity of 3.43 km/s. Only possibilities (4) and (5) are in accord with the observations of the present study. Since the station and blast positions were known within ± 100 m the more likely explanation is that the residuals are due to velocity changes in the upper crust. Because of the small distances between stations over the first 68 km of the LCK profile, it is unlikely that the changes in velocity occur at any significant depth, and consequently they must be

localised near surface effects. The velocity ratio of 1.72 for P to S velocities corresponds to a Poissons ratio of 0.24.

A set of eight S-wave arrivals have been read from records between 120 and 230 km. The travel time equation for these eight arrivals is equation (13).

Table 4.5 Travel Time Equations for Shear Waves - LCK profile

PHASE	TRAVEL TIME EQUATION	NO OF DATA USED	RMS RESIDUAL	
S1	$t = \frac{x}{(3.43 \pm 0.05)} + 0.41 \pm 0.21$	10	0.23	(12)
Sn	$t = \frac{x}{(4.45 \pm 0.04)} + 12.92 \pm 0.36$	8	0.16	(13)

4.4.2 Iron Baron Profile

The S1 arrivals which were recorded along the IB-E profile were both few in number and poor in quality, in contrast with the arrivals recorded on the LCK profile at similar distances. This may have been a result of the delayed firing of the shots at IB. The arrivals which were detected were, in general, consistent with the travel time equation for the LCK arrivals.

Between 107 and 289 km from IB, however, S wave arrivals were clearly recorded, and 23 arrival times were

read in this distance range. The linear travel time equation which fits these arrivals is

$$t = \frac{\Delta}{(4.43 \pm 0.03)} + 13.0 \pm 0.29 \qquad (14)$$

The RMS residual of the data from this equation is 0.33 sec, which reflects the difficulty of accurately locating S wave onsets. It is clear that the apparent velocity of these Sn arrivals agrees with that for the corresponding arrivals on the LCK profile, thus confirming that the arrivals are probably Sn.

4.4.3 Comments

The apparent velocity and intercept terms of equations (14) and (13) are appropriate for the phase Sn, in which case the shear wave velocity in the upper mantle is seen to be lower than any value previously determined in South Australia (see Table 1.1). Using the Pn velocity determined above, the velocity ratio v_p/v_s is equal to 1.79. In order to evaluate the depth to the mantle from equations (13) and (14), it is necessary to adopt a model for the S wave velocity structure of the overlying crust. If a uniform crust is assumed with S1 velocity equal to 3.43 km/s, as determined from equation (12), then the depth to the Moho is approximately 35 km. If, however a deep crustal layer corresponding to that having a P wave velocity of 6.46 km/s also exists for S waves, then the S velocity in the lower crustal would be 3.76 km/s, assuming $v_p/v_s = 1.72$ in the

lower crust as for the upper crust. When this two layered crustal model is used to calculate the depth to the Moho a value of 39 km is obtained, which is in agreement with the depth to the Moho obtained from the P wave travel times. It should be noted that no S wave arrivals from the lower crust have been identified from the records of either the IB or LCK profiles.

4.5 Summary of Findings

A model has been obtained which describes the variation of seismic velocity with depth in the Adelaide geosyncline. A distinguishing feature of the new crustal model is a first order discontinuity of velocity which is located at a mean depth of 18 km in the crust. Although such a discontinuity has been found in other parts of the continent, and several workers have assumed its existence for the whole of the Australian continent, none of the earlier studies conducted in South Australia had found evidence for such a discontinuity. In the present survey, evidence for the discontinuity's existence has been obtained from both refraction and reflection data.

The crustal model has the following additional features:

(a) Over much of the Adelaide geosyncline the near surface and outcropping rocks of the Adelaidean sediments have a P wave velocity of 4.8 km/s. The mean velocity in the upper crustal layer is 5.95 km/s, and in the lower crustal layer the velocity is 6.46 km/s. The velocity of P waves in the

material immediately below the Moho is 7.97 km/s. As is evidenced from the good agreement between the apparent velocity of refracted arrivals and the average velocity of reflected arrivals, the two crustal layers are essentially uniform. Furthermore, the velocity in the Adelaidean sediments increases rapidly with depth to attain a value near that typical of the upper crust within a kilometre or two from the surface.

(b) The mean depths to the intermediate and Moho discontinuities are respectively 18 and 39 km to the nearest kilometre. Depths to both horizons vary by up to 5 km from these mean values. The intermediate discontinuity appears to increase in depth by 4 to 5 km at the eastern edge of Spencer Gulf, approximately following the contour of magnetic basement. Arrivals refracted at the Moho indicate that the Moho probably occurs at shallower depths than the average in a region bounded by the Chace and Druid Ranges in the north and the Willochra Basin in the west. This uplift probably extends no further south than latitude 33°S. Pn data also suggest that the Morgan Fault is associated with a major basement feature, since the Morgan Fault corresponds to a markedly reduced time term for Pn arrivals as the fault is crossed from west to east.

(c) No evidence has been found for the existence of a low velocity layer in the crust.

(d) The mean shear wave velocities in the upper crust and mantle are 3.43 and 4.45 km/s respectively.

APPENDIX A

INTERPRETATION METHODS

A.1 On the Validity of Geometric Ray Theory

The raw data obtained from seismic recordings consist of arrival times and possibly amplitudes and frequencies of seismic waves which have travelled by various paths from source to receiver. These, together with the distance between source and receiver are used to deduce a model of the velocity distribution within the crust, which may subsequently be interpreted in terms of sub-surface structure. Most commonly, the analysis of seismic data assumes that geometric ray path theory suitably describes the propagation paths of seismic energy, and that plane wave reflection and refraction coefficients are appropriate for computing the amplitudes of seismic phases.

In a medium where the velocity varies with depth, it has been shown (e.g. Grant and West (1965)) that the WKBJ plane wave approximation yields a solution of the displacement wave equations, which reduces to the geometric ray path description, provided that the wave frequencies involved are large compared with any velocity gradients in the medium i.e. $|dc/dz| << 2\pi f$. In the case of the recording equipment for which the lower 3 dB point occurs at a frequency of 2Hz (filter 2) the condition is that $|dc/dz| << 12$ approximately. In view of the range of velocities and velocity contrasts to be expected in the crust, such large

gradients could only exist in very thin transition zones, fractions of a wavelength thick, but White (1967) has shown that a transition zone less than $\lambda/10$ thick may be expected to behave as a reflecting and refracting discontinuity. Thus ray theory may be thought to apply throughout the crust, with possible exceptions being in the near surface low velocity material, where velocity increases rapidly with depth as a result of increased pressure and decreased porosity of the cover material, and in the vicinity of the Moho and other velocity discontinuities which may occur in the crust. These regions of rapid velocity change may be expected to act as sharp discontinuities for the wavelengths being observed.

For homogeneous and isotropic media, geometric ray theory and plane wave reflection coefficients are the first approximations to a formal solution of the elastic wave problem. Cerveny (1966) has shown, however, that although, over some distance ranges from the source, the geometric ray theory gives relatively exact results, in other regions the validity of the formulae of geometric ray theory is only limited, and that this is most apparent in the region of critical reflection. His results are important for the understanding of both kinematic and dynamic properties of seismic waves. In the first place, the sharp peak of amplitude for reflected phases, which is expected, from geometric ray theory, to occur at the critical distance, is found to be a smooth peak which occurs as much as 50 km beyond the critical distance for waves reflected from the Moho. The offset distance of the observed peak from that

calculated from geometric ray theory, is a function of frequency and velocity contrast at the reflector, being greater for both lower frequencies and smaller velocity contrasts. The importance of this result is that it calls into question the practice of associating large amplitudes with the critical distance, which has been used as a discriminator between hypothetical crustal models derived from travel time data (e.g. Steinhart and Meyer (1961)).

Cerveny also determined that the amplitudes of pure head waves are very small in comparison to the amplitudes of reflected waves, but that small velocity gradients in the lower medium can markedly strengthen the amplitudes of head waves, even to exceed the amplitudes of the reflected waves, beyond a certain distance from the source. Furthermore, the true critically refracted (head wave) arrivals define a branch of the travel time curve which is not tangential to the curve for the corresponding reflected waves, as expected from geometric ray theory, but which in fact intersects it. The point of intersection of the two curves corresponds to the point of maximum observed amplitude for the reflected waves. It would appear from his Figure 5, however, that the difference between his more exact travel time curves, and those determined from geometric path methods, is smaller than the residuals of the data commonly encountered in long range refraction profiles, so that without very detailed profiling and accurate travel time data, geometric ray theory will give a sufficiently accurate account of the travel times in most surveys.

A.2 On the Inversion of Travel Times

Several methods exist for determining velocity distributions from travel time data, but the use of a particular method depends on the nature of the survey which provided the data. Generally, refraction data are interpreted in terms of a layered model of the crust. In the majority of early refraction work, crustal velocities and the thicknesses of crustal layers were obtained explicitly from the slopes and intercepts of straight line graph segments defined by first arrivals plotted on a time-distance graph. However, Green and Steinhart (1962) criticized the sole use of first arrivals and advocated the use of later arrivals and their amplitude characteristics, to provide information on the velocity contrasts at discontinuities in the crust. In addition, Tuve, Tatel and Hart (1954) showed that a large number of possible velocity-depth models can be found which fit a given set of first arrivals equally well.

Alternative interpretation schemes such as the time-depth method of Hawkins (1961), which was used to analyse the TASS survey results (Finlayson *et al* (1974)), and the refraction methods traditionally used in geophysical prospecting, require approximate in-line, reversed profiling. Whilst the time term method of Willmore and Scheidegger (1957) avoids this constraint, the method does require the location of at least one receiver at one shot point for unambiguous derivation of the station and shot time terms. The time

terms enable the depth to the refractor to be calculated in the vicinity of each of the shot and recording points. If the structure above the refractor is not known, but assumed to be constant over the region of interest, then absolute depths are not known, but variations of depths to the refractor can be recognised from relative variations of the time terms from point to point. In an extension of the method, Bamford (1976) introduced a means of reducing the number of time terms to be found for a large number of otherwise independent shot and recording points, by grouping shot and receiver points into areas according to regional trends of surface geology or Bouguer gravity anomaly. Each area is then assigned a particular value of the time term, thus reducing the number of variables. One further difficulty with non-linear profiling would seem to be that of determining whether arrivals at different stations had arisen from the same, or different refracting horizons. This difficulty is not so great in the case of in-line profiling where phases can be "followed" along the profile thus enabling newly emerging phases to be identified as such.

Hall (1964) described a method for using converted waves to deduce crustal structure. The method is potentially a very powerful one since, for a single layered crust over a refractor, the observation of three different head waves at a single station, and for a single shot, enables both the marker velocity and the depths to the marker beneath both shot and station points to be calculated. Unfortunately, the identification of converted head waves is

a major obstacle to the use of this method, as evidenced by the general lack of reports of such phases in the literature.

Since the advent of high speed computers it has become possible to easily compute travel times and amplitudes of seismic phases for any postulated crustal structure. White (1967) has constructed a programme (CRVV) to compute travel times and free surface amplitudes for the phases Pl, PR, Pn, Sl, SR, Sn, SmP and sPR as well as converted head waves, for a crust and upper mantle having any number of layers, in which the velocity can vary with depth. With this powerful tool, calculated data can be compared to observed data, and the crustal model altered until the agreement between theory and experiment reaches a required level. This is the essence of the inversion method of Braille (1973).

Bessonova et al (1974) have developed a method (the Tau method) for determining the envelope of possible velocity-depth curves, which might be obtained by the inversion of a given set of travel time data. The method, as it first appeared, was amenable to Deep Seismic Sounding data i.e. from surveys with very high station densities along the profile, and very good time control. Small station spacings (approx. 1 km) enabled the travel time curve to be smoothed by averaging over 5 km intervals. In a second paper (Bessonova et al (1976)) the Tau Method was extended to the problem of inverting earthquake data, by using statistical methods to obtain limits on the Tau function. Bates and Kanasewich (1976) applied the Tau method to data from the

long range Seismic Project Early Rise. The main advantage claimed for the Tau method by Bessonova et al is the relative objectivity of the method, compared with other available inversion schemes.

In spite of these many inversion schemes with their varying degrees of sophistication, it should be remembered that all crustal models must be regarded as approximations and indicative of average crustal velocities. Sometimes additional geophysical data may be useful in distinguishing between models, but "when there is no such evidence, and there are no statistical differences in the fit to the data produced by various models, then the only justifiable choice is the simplest model" (White (1967)). This has been the underlying philosophy of the present refraction programme.

APPENDIX B

TRAVEL TIMES OF PHASES OBSERVED ON THREE PROFILES

The following tables contain the travel times of all phases used in the present study, together with the stations at which the phases were observed and the distance of each station from the seismic source. The station code names may be related to sites shown in Figures 4.1 and 4.3. An R following a travel time indicates that the phase was interpreted as a reflected phase.

B.1 Leigh Creek Profile

STATION	DISTANCE	TRAVEL TIME (SEC)			
	(km)	P1	P2/P2R	Pn/PnR	S1/Sn
L01	6.78	1.09			2.09
L02	11.02	2.09			
L03	17.64	3.17			
L04	22.62	3.92	7.17 R		6.92
L05	24.88	4.61			8.11
L06	29.28	5.24	8.02 R		9.17
L07	34.50	6.02	8.53 R		10.57
L08	37.54	6.49	8.98 R		11.24
L09	44.17	7.59			13.09
L10	57.70	9.81	11.67 R		16.94
L11	61.76	10.54	12.02 R		18.29
L12	68.49	11.84			20.59
L13	80.01	13.69	14.94 R		
L14	87.64	14.90	16.02 R		
L15	95.63	16.23	17.25 R	19.73 R	
L16	99.29	17.21	17.85 R		

B.1 Leigh Creek Profile (ctd)

STATION	DISTANCE	TRAVEL TIME (SEC)			
	(km)	P1	P2/P2R	Pn/PnR	S1/Sn
L17	103.85	17.76	18.56 R	20.86 R	
L18	107.32	18.04			
L19	118.98	20.28	21.04 R	22.63 R	39.75
			20.68		
L20	122.20		21.71 R		
L21	133.69		22.91	24.75 R	
L22	135.76		23.37	25.0 R	43.25
L23	144.75		24.99	25.89	
				26.35 R	
L24	152.89		26.45 R	26.95	47.2
				27.48 R	
L25	157.58		26.99	27.64	
				28.04 R	
L26	159.46		27.16	27.71	
L27	166.41		28.23		50.63
L28	179.86	30.56	30.26	30.26	53.5
				31.56 R	
L29	202.46			32.63	58.23
L30	209.95	35.40	34.90	33.65	60.0
L31	226.59	38.16	37.68	35.73	64.0
L31	226.86		37.66	35.78	
L32	231.38	39.06	38.06	36.36	
L33	238.79			37.00	
L34	252.43			38.70	
L35	265.65			40.73	
L36	277.14			41.90	
L37	277.77			42.27	

B.1 Leigh Creek Profile (ctd)

STATION	DISTANCE (km)	TRAVEL TIME (SEC) P1	P2/P2R	Pn/PnR	S1/Sn
B23	320.35			47.58	
B25	321.92			47.65	
L40	331.14			49.34	

B.2 Iron Baron Profile - Iron Baron Blasts

B01	2.33	0.61			
B02	7.29	1.26			
B03	8.62	1.64			
B04	14.14	2.60	3.75		
B05	16.21	3.06			
B06	19.01	3.35	4.30		
B07	21.69	4.09			
B08	24.04	4.29			
B08	24.80	4.45			
B09	29.69	5.19	5.69		
B10	32.79	5.83	6.19		
B11	78.44	13.44			
B12	91.48	15.68			
B13	101.49	17.26			
B14	104.30		17.87		
B15	107.52		18.27	21.27	37.33
B16	110.87		19.22		38.47
B17	114.54		19.72		
B18	121.44		20.39	23.09	40.64
B19	125.31		20.95	23.45	40.95
B20	133.49		22.34		43.34

B.2 Iron Baron Profile (ctd)

STATION	DISTANCE	TRAVEL TIME (SEC)			
	(km)	P1	P2/P2R	Pn/PnR	S1/Sn
B20	134.24		22.49		43.37
B21	139.89		23.19	25.44	44.19
B21	140.63		23.34	25.34	44.34
B22	145.02		24.03	26.16	45.78
B22	145.78		23.99		45.99
B22	145.78		24.08		
B23	148.67		24.48	26.73	
B23	149.43		24.59	26.59	
B24	156.67		26.06	27.49	48.81
B25	161.73		26.51	27.96	49.64
B26	166.30			28.44	50.94
B27	165.98		27.39	28.56	50.27
HTT	170.68			28.74	51.12
HTT	170.68		28.17	29.30	
HTT	170.68		28.05	29.04	
B28	177.40		29.39	30.02	53.14
B29	181.89		29.77	30.52	54.77
B30	190.65		31.18	31.68	56.18
B31	195.43		31.94	32.34	
B32	205.43			33.51	
B33	212.99			34.45	
B33	212.99			34.81	60.60
B34	215.95			35.4	61.77
B35	222.81			36.03	
B35	222.81			35.81	
B36	227.73			36.51	
B37	241.08			37.97	67.22

B.2 Iron Baron Profile (ctd)

STATION	DISTANCE (km)	TRAVEL TIME (SEC) P1	P2/P2R	Pn/PnR	S1/Sn
B38	248.46			38.91	
B39	256.38			40.17	
B40	288.73			44.05	78.55
B41	316.38			47.13	
B42	355.58			51.89	
B43	359.90			52.33	
B44	365.29			52.47	

B.3 Iron Baron Profile - Iron Monarch Blasts

B10	51.48	8.90			
B18	134.34	22.37		25.03	
B19	137.78	23.32		25.07	
B22	157.50	25.71		27.46	
B23	161.11	26.35		27.86	49.48
B24	168.94	28.20		28.95	
B25	173.90	28.43		29.38	
B31	206.51			33.16	
B30	203.21			32.95	
B33	224.85			35.99	
B35	234.57			37.16	65.91

B.4 Kanmantoo Profile

K00	1.56	0.30			
K01	3.32	0.58			
K02	4.30	0.87			

B.4 Kanmantoo Profile (ctd)

STATION	DISTANCE	TRAVEL TIME (SEC)			
	(km)	P1	P2/P2R	Pn/PnR	S1/Sn
K03	6.10	1.13			
K04	7.54	1.47			
K05	9.61	1.84			
K06	14.14	2.54			
K07	14.33	2.71			
K08	15.68	2.92			
K09	16.99	2.90			
K10	18.70	3.48			
K11	27.99	4.55			
K12/ADE	29.55	5.53			
K13	36.37	6.07			
K14	43.49	8.18			
K14	43.49	8.04			
K15	102.1	17.2			
B41	178.32		29.79		
HTT	184.35		30.54		
B29	191.60		31.83		
B27	193.13		31.78		
B21	203.86		33.63		
B20	204.31		33.56		
L31	291.62		47.4		
L30	308.0		50.09		

B.5 Miscellaneous Events

B.5.1. Leigh Creek Blasts

STATION	DISTANCE (km)	TRAVEL TIME (SEC)		
		FIRST ARRIVAL	Pn	S ARRIVAL
Willochra	180.33	30.03	30.29	
B04	310.01		46.56	
B06	310.03		46.65	

B.5.2 Iron Baron Blasts

BN1	38.31	6.54		
BN2	43.61	7.52		
BS1	87.88	14.51		
L07	269.54		41.51	73.64
L09	261.62		40.57	74.32
L18	223.86		35.77	63.77
L21	202.87		33.54	60.29
L20	211.70		34.71	62.09
L21	202.87		33.28	59.03
Arkaba	178.92		30.76	55.51
L28	174.48		29.59	51.72
Hwkr 00	172.17		29.25	51.75
L29	161.33	26.85	27.85	49.65
L30	158.62	26.70	27.50	47.08
L32	153	25.84		
L31	152.8	26.01	27.14	
L32	152.24	25.59	26.97	46.84
06N	147.97	25.51	26.39	46.31
L31	151.31	25.26	26.50	

B.5.2. Iron Baron Blasts (ctd)

STATION	DISTANCE (km)	TRAVEL TIME (SEC)		
		FIRST ARRIVAL	Pn	S ARRIVAL
Oladdie 1	150.61	25.42	26.42	44.67
L34	147.64	24.52	25.77	45.27
03S	145.29		25.85	46.48
06S	148.0	24.99	26.49	
L35	149.0	25.07	26.45	45.70
L37	144.18	24.19	25.32	45.69
Black Rock	150.40	25.01		46.01
Peterborough	144.39	24.41	26.16	
Minvalara	148.17	25.44	26.69	46.19
Willochra	143.06	23.28		
Yongala	151.51	25.07	26.37	46.27
S1	206.86		34.52	61.0
S1	206.86		34.68	61.2
S3	244.64		40.57	
S4	243.31		39.94	69.24

B.5.3. Iron Monarch Blasts

L12	221.77		35.82	63.95
L29	150.62	24.81	26.31	47.31
06S	149.0	24.83	26.08	
L32	146.65	24.70		
L34	146.10	24.54	25.57	
06N	144.04	24.38	25.58	
03S	145.04	23.81	25.31	
S1	229.99		37.08	

REFERENCES

Bamford D. (1976) Mozaic Time - Term Analysis Geophys. J. R. astr. Soc. 44

Bates A., Kanasewich E. (1976) Inversion of seismic travel times using the Tau method Geophys. J. R. astr. Soc. 47

Bessonova E.N., Fishman V.M., Ryaboyi V.Z., Sitnikova G.A. (1974) The Tau Method for Inversion of Travel Times Geophys. J.R. astr. Soc. 36 377

Bessonova E., Fishman V., Shnirman M., Sitnikova G. (1976) The Tau Method for Inversion of Travel Times - II Earthquake data Geophys. J. R. astr. Soc. 46

Bolt B.A., Doyle H.A., Sutton D.J. (1958) Seismic observations from the 1956 Atomic Explosions in Australia Geophys. J. Roy astr. Soc. 1 No. 2

Braille L. (1973) Inversion of Seismic Reflection and Refraction Data J. Geophys Res. 78

Branson J., Moss F., Taylor F. (1972) Deep Crustal Reflection Seismic Test Survey, Mildura, Victoria and Broken Hill, N.S.W. 1968 Bur. Min. Resource. Aust Rec., 1972/127

Cerveny V. (1966) On Dynamic Properties of Reflected and Head Waves in the n-layered Earth's Crust Geophys J. R. astr. Soc. 11

Cleary J. (1967) P times to Australian stations from nuclear explosions B.S.S.A. 57 No. 4 773

Cleary J.R., Simpson D.W. (1971) Seismotectonics of the Aust. continent. Nature 230 239

Cleary J.R., Simpson D.W., Muirhead K.T. (1972) Variations in upper mantle structure from observations of the Cannikin explosion Nature 236 111

Cleary J. (1973) Australian crustal structure Tectonophysics 20 241

Cook P.J. (1966) Rec. Bur. Min. Res. Geol. Geophys. Austral. 46

Crawford A.R. (1970) Economic Geology 65 11

Denham D., Simpson D.W., Gregson P.J., Sutton D.J. (1972) Travel times and amplitudes from explosions in Northern Australia Geophys J. Roy. astr. Soc. 28 225

Dooley J.C. (1970) Seismological studies of the Upper Mantle in the Australian Region. Proc. 2nd Symp. Upper Mantle Project Hyderabad

Doyle H.A., Everingham I.B. (1964) Seismic velocities and crustal structure in Southern Australia. J. Geol. Soc. Aust. 11 141

Doyle H.A., Everingham I.B., Sutton D.J. (1968) Seismicity of the Australian continent J. Geol. Soc. Aust. 15 295

Finlayson D.M., Cull J.P., Drummond B.J. (1974) Upper Mantle structure from the trans Australian seismic survey (Tass) J. Geol. Soc. Aust. 21 447

Gough D.I., McElhinny M.W., Lilley F.E. (1974) A Magnetometer Array study in Southern Australia Geophys. J. Roy. astr. Soc. 36 345

Grant F.S., West G.F. (1965) Interpretation theory in Applied Geophysics McGraw-Hill

Green R., Steinhart J.R. (1962) On crustal structure deduced from seismic time distance curves New Zealand J. Geol. & Geophysics 5 579

Gutenberg B., Richter C.F. (1954) Seismicity of the Earth and associated phenomena (2nd ed.) Princeton Univ. Press, New Jersey

Hales A.L., Doyle H.A. (1967) P & S travel time anomalies and their interpretation. Geophys. J. Roy. astr. Soc. 13 403

Hales A.L., Nation J.B. (1973) A Seismic Refraction Survey in the Northern Rocky Mountains Geophys. J.R. astr. Soc. 35

Hall D.H. (1964) Converted waves in refraction surveys over markers with variable depth. Geophysics 29 733

Hawkins L.V. (1961) The Reciprocal Method of routine shallow seismic refraction investigations. Geophysics 26 806

Hawkins L.V., Hennion J.F., Nafe J.E., Doyle H.A., (1965) Deep Sea Res. 12 479

Herrin E. et al (1968) Seismological Tables for P Phases B.S.S.A. 58

Jaeger J.C. (1970) Heat flow and radioactivity in Australia. Earth Planet. Sci. Lett. 8 285

Jeffreys H. (1962) The Earth Cambridge Press

Kendall G. (1967) Reconnaisance seismic refraction survey in the South Australian portion of the Eucla Basin, 1964 Min. Rev., Adelaide 122

Kosminskaya I.P., Riznichenko T.V. (1964) Seismic studies of the Earth's crust in Eurasia, in Research in Geophysics 2 81

Ludbrook N. (1961) Sub-surface stratigraphy of the Maralinga area, South Australia. Trans R. Soc. S. Aust 84

McElhinny M.W. (1973) Earth Sciences and the Australian Continent Nature 246 264

McEvilly T. (1966) Crustal Structure Estimation within a large Scale Array Geophys. J. R. astr. Soc. 11

Milton B. (1974) Experimental seismic exploration, eastern Eucla Basin, South Australia. Quarterly Geological Notes 52

Milton B. (1974) Seismic experiments in the northern Eucla Basin, South Australia. Quarterly Geological Notes 51

Milton B. (1975) Reconnaissance seismic exploration, southwest Arekaringa Basin, South Australia, 1974. Quarterly Geological Notes 53

Landisman M., Mueller S. (1966) Seismic studies of the earth's crust in continents 1. Evidence for a low velocity zone in the upper part of the lithosphere Geophys. J. Roy. astr. Soc. 10 525

Muirhead K., Cleary J., Finlayson D. (1977) A Long Range Seismic Profile in southeastern Australia. Geophys. J. R. astr. Soc.

Parkin L.W. (1969) ed. Handbook of South Australian Geology S.A. Govt. Printer

Press in Handbook of Physical Constants

Willmore P.L., Scheidegger A.E. (1957) The use of a least squares method for the interpretation of data from seismic surveys. Geophysics 22 9

Steinhart J.S.,Meyer R.P. (1961) Explosion studies of Continental Structure Publ. Carneg. Inst. Washington 622

Stewart I.C.F. (1971) Seismic activity in 1969 associated with the eastern margin of the Adelaide Geosyncline. J. Geol Soc. Aust. 18 143

Stewart I.C.F. (1972) Seismic interpretation of crustal structure in the Flinders-Mt. Lofty ranges and gulf regions, South Aust. J. Geol. Soc. Aust. 19 351

Tammemagi A.Y., Lilley F.E.M. (1973) A magnetotelluric traverse in Southern Australia. Geophys J. Roy astr. Soc. 31 433

Tuve M.A., Tatel H.E., Hart P.J. (1954) Crustal structure from seismic exploration J. Geophys. Res. 59 415

White R.E. (1969) Seismic phases recorded in South Australia and their relation to crustal structure Geophys. J. Roy astr. Soc. 17 249

Willmore P., Bancroft A. (1961) The Time - Term approach to Refraction Seismology Geophys. J. R. astr. Soc. 4

White R.E. (1967) Ph.D. Thesis, University of Adelaide (unpublished)

Herrin E., Taggart J.N. (1968) Regional variations in P travel times B.S.S.A. 58 1325

Wilson J.T. (1968) in Science, History and Hudson Bay, ed. Beals C.S. 2 (Queen's Printer, Ottawa).